Advances in the engineering of the outer blood-retina barrier: From in-vitro modelling to cellular therapy

Chloé Dujardin, Walter Habeler, Christelle Monville, Didier Letourneur, Teresa Simon-Yarza

Bioactive Materials 31 (2024) 151–177

Contents lists available at ScienceDirect

Bioactive Materials

journal homepage: www.keaipublishing.com/en/journals/bioactive-materials

Review article

Advances in the engineering of the outer blood-retina barrier: From in-vitro modelling to cellular therapy

Chloé Dujardin [a,*], Walter Habeler [b,c,d], Christelle Monville [b,c], Didier Letourneur [a], Teresa Simon-Yarza [a,**]

[a] Université Paris Cité, Université Sorbonne Paris Nord, Laboratory for Vascular Translational Science (LVTS) INSERM-U1148, 75018 Paris, France
[b] INSERM U861, I-Stem, AFM, Institute for Stem Cell Therapy and Exploration of Monogenic Diseases, 91100, Corbeil-Essonnes, France
[c] U861, I-Stem, AFM, Université Paris-Saclay, Université D'Evry, 91100, Corbeil-Essonnes, France
[d] CECS, Centre D'étude des Cellules Souches, 91100, Corbeil-Essonnes, France

ARTICLE INFO

Keywords:
Outer-blood retina barrier
Tissue engineering and cellular therapy
In-vitro disease modelling
3D complex models

ABSTRACT

The outer blood-retina barrier (oBRB), crucial for the survival and the proper functioning of the overlying retinal layers, is disrupted in numerous diseases affecting the retina, leading to the loss of the photoreceptors and ultimately of vision. To study the oBRB and/or its degeneration, many *in vitro* oBRB models have been developed, notably to investigate potential therapeutic strategies against retinal diseases. Indeed, to this day, most of these pathologies are untreatable, especially once the first signs of degeneration are observed. To cure those patients, a current strategy is to cultivate *in vitro* a mature oBRB epithelium on a custom membrane that is further implanted to replace the damaged native tissue. After a description of the oBRB and the related diseases, this review presents an overview of the oBRB models, from the simplest to the most complex. Then, we propose a discussion over the used cell types, for their relevance to study or treat the oBRB. Models designed for *in vitro* applications are then examined, by paying particular attention to the design evolution in the last years, the development of pathological models and the benefits of co-culture models, including both the retinal pigment epithelium and the choroid. Lastly, this review focuses on the models developed for *in vivo* implantation, with special emphasis on the choice of the material, its processing and its characterization, before discussing the reported pre-clinical and clinical trials.

1. Introduction

The blood-retina barrier (BRB) is an essential component for the maintenance of the retinal functionality. Its integrity is indispensable for the ocular immune privilege. Typically, the BRB is subdivided into the inner (iBRB) and the outer (oBRB) barrier. The iBRB is composed of endothelial cells that line the retinal vasculature which originates from the central retinal artery and supplies the inner retinal layers [1]. The oBRB is the outermost structure of the retina, located under the photoreceptors layer, and is composed of three distinct layers: the retinal pigment epithelium (RPE), the Bruch's membrane (BM) and the choroid being responsible for the vascularization of the outer layers of the retina (Fig. 1). In numerous retinal diseases, the oBRB is disrupted due to the formation of extracellular aggregates, neovascularization, or genetic mutation(s) altering the epithelium functions, as in dry age-related advanced macular degeneration, in diabetic macular edema or in retinitis pigmentosa, respectively (Fig. 1). This leads to a complete degeneration of the epithelial layer, followed by a loss of the overlying photoreceptors and, ultimately, to vision loss. To this day, no efficient treatment is available for the patients, especially once the first signs of degeneration are observed.

Due to its location, the oBRB is difficult to study *in vivo*. Thus, many *in vitro* models have been designed in the last three decades to model the oBRB and study the complex cellular mechanisms and interactions in the tissue. With the rise of induced pluripotent stem cells (iPSCs) since the 2010's, *in vitro* models have also been recently developed to investigate disease mechanisms and potential therapeutic strategies, both to prevent, reduce and/or treat the disease symptoms. To cure patients already

Peer review under responsibility of KeAi Communications Co., Ltd.
* Corresponding author.
** Corresponding author.
E-mail addresses: chloe.dujardin@inserm.fr (C. Dujardin), teresa.simon-yarza@inserm.fr (T. Simon-Yarza).

https://doi.org/10.1016/j.bioactmat.2023.08.003
Received 5 June 2023; Received in revised form 13 July 2023; Accepted 6 August 2023

displaying signs of degeneration, several strategies are currently being investigated and were recently reviewed by Cehajic-Kapetanovic et al. [2]. Among those, one promising strategy to cope with the vision loss is cellular therapy. Several groups have investigated the injection of a RPE cellular suspension [3,4]. However, the RPE layer being tightly organized and polarized, the injected cells were poorly integrated in the patient tissue and could not properly fulfil their functions. To improve the cellular therapy outcome, the current strategy is to cultivate a RPE layer on a biomaterial, either natural or synthetic, and to perform a subretinal implantation of the cell sheet with the material. In this case, the cells would already be organized upon implantation, favouring their integration in the native oBRB. For this strategy, various material and cell sources have been proposed in the last 30 years, leading to five on-going clinical trials.

In this review, after a brief description of the oBRB and the studied diseases, we give a historic overview of the advances in oBRB models, from the simplest including solely the RPE to the more complex ones that model both the RPE and the choroid. From this, we discuss the choice of the cell type to model the oBRB, from immortalized cell lines to cells derived from stem cells passing through primary cells. The models are then examined in terms of culture material characteristics, by considering separately the models designed for *in vitro* versus *in vivo* applications, due to their different material requirements.

2. Biology of the oBRB and the main associated diseases

2.1. Outer blood-retina structure

Each component of the oBRB fulfils specific functions. The RPE, thoroughly described by Strauss [5], is composed of a monolayer of polarized pigmented cells connected by tight junctions. Its apical membrane faces photoreceptor outer segments (POS) whereas the basolateral membrane faces the BM. The RPE performs several crucial functions for the homeostasis of the photoreceptors. First, thanks to its pigmentation, the RPE helps scattered light absorption and protects the retina from photo-oxidative damage. Nonetheless, one inevitable light damage is the accumulation of photo-damaged proteins and lipids in the POS, leading to a need for their constant renewal, conducted by the RPE cells via POS phagocytosis. Moreover, the RPE is responsible for trans-epithelial transport, in both directions: from blood to subretinal space (glucose and other nutrients, retinal small molecule, fatty acids) and from the subretinal space to the blood (water, metabolic end-products such as lactic acid, ions). The RPE is thus responsible of the ion composition in the subretinal space. The RPE is also involved in the visual cycle and notably in the recycle of one key molecule in maintaining photo-receptors excitability, the retinal. Finally, some growth and structural factors such as vascular endothelial growth factor (VEGF)

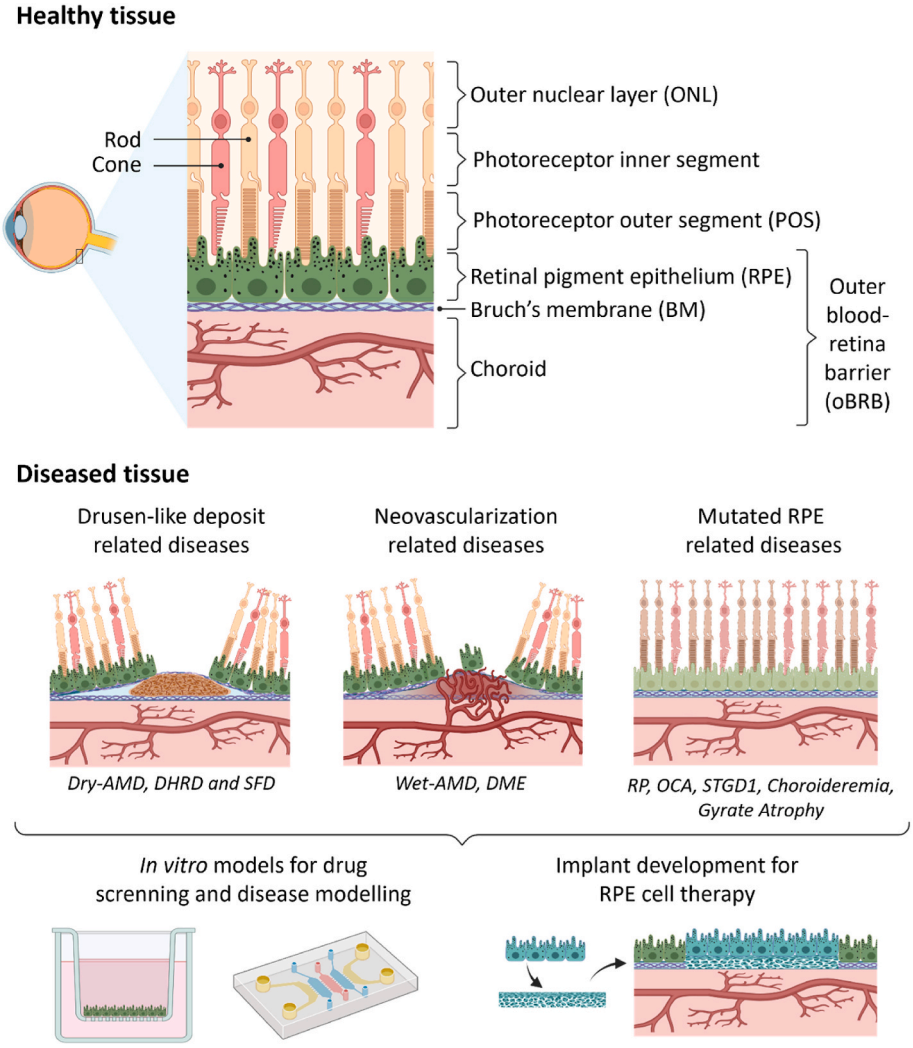

Fig. 1. Schematic representation of the photoreceptors and the oBRB organization in the retina (top) and of the 3 major types of damage that can be observed in retinal diseases (middle) with an overview of the types of oBRB model that have been developed to study and treat them (bottom). Figure created with *BioRender.com*.

and pigment epithelium derived factor (PEDF) are secreted by the RPE cells, in a polarized manner, notably influencing choroidal endothelial cells behaviour.

The choroid, well described by Nickla & Wallman [6], is a vascularized layer supplying the outer layers of the retina. It is characterized by fenestrated capillaries with a gradient of diameters, from 20 μm to 40 μm diameter, near the RPE layer, to vessels with a maximum diameter of 200 μm at the extremity of the choroid [7]. Within the choroid, three main layers are distinguished: the choriocapillaris, the Sattler's vascular layer with medium vessels and the Haller's vascular layer with large vessels. The entire thickness of the choroid decreases with age, from 200 μm at birth to approximatively 90 μm at 90 years old. In addition to its blood supplier role, the choroid is responsible for the thermoregulation, the control of the intraocular pressure, the adjustment of the retina position, the drainage of the aqueous humour and the secretion of multiple growth factors, as part of its numerous interactions with the RPE.

Separating the choroid from the RPE monolayer, the BM is a thin (2–4 μm in thickness) acellular membrane [8]. The BM possesses a pentalaminar structure divided upon, from the inner to the outer sides: the RPE basement membrane, the inner collagenous zone, the elastic layer, the outer collagenous zone and finally, the choriocapillaris basement membrane [6,9]. The BM is mainly composed of collagen, notably types I and IV, laminin, elastin and fibronectin, with a composition varying between the different layers and with age. Given its strategic location, the BM plays a crucial role in molecules exchanges, notably oxygen, nutrients, waste and cell-cell communication molecules, and for the cellular behaviour notably differentiation and proliferation. Moreover, BM composition and structural modifications are observed in many pathological processes [9,10].

2.2. Diseases affecting the oBRB

Due to ageing or to genetic alterations, the structure and the functionality of the oBRB can be altered, leading to a loss of photoreceptors and ultimately of vision. Importantly, in some cases, the onset of the disease is due to a genetically-driven degeneration of the photoreceptors that leads to alterations in the oBRB that will further aggravate the initial photoreceptor pathology [11]. We here present several diseases having been modelled.

- Age-related macular degeneration

Age-related macular degeneration (AMD) is a progressive blinding disease affecting approximately 170 million individuals globally, making it a leading cause of visual disability in the world, especially in the developed countries. Since the principal risk factor is age, the prevalence of AMD is anticipated to increase in the next decades, reaching 288 million by 2040, due to the global aging of the population [12].

Two forms of AMD are distinguished: the "dry", or atrophic, and the "wet", or exudative. The "dry" form is characterized by an accumulation between the RPE and the choroid of insoluble aggregates called drusens, made of lipids and proteins. Disrupting the communication between the RPE and the choroid, these drusens lead to the loss of the RPE cells and consequently to a loss of photoreceptors [13]. Only one treatment, Syfovre, based on pegcetacoplan injection, developed by Apellis Pharmaceuticals and recently approved by the FDA, exists against dry AMD.

The "wet" AMD, less prevalent with, in average, 15% of the cases, is caused by a neo-vascularization of the choroid. These neo-vessels penetrating through the BM lead to local destruction of the RPE and the photoreceptors of the macular region of retina, with the consequent loss of central vision. The causes for this neo-vascularization are still unclear but it is thought to be the response to an oxidative stress, leading to an abundant production of VEGF by the RPE [14]. If detected early, wet AMD can be treated with anti-angiogenic drugs such as bevacizumab. However, in later stages of the disease, the BM and RPE disruption are to this day irreversible.

- Diabetic macular edema

Diabetic macular edema (DME) is the main retinal vascular complication of diabetes, making it the main cause of blindness for people younger than 65 years old [15]. DME is characterized by a disruption of both parts of the BRB with the onset of the disease usually localized in the inner BRB, leading to an accumulation of fluid within the intraretinal layers of the macula. In the oBRB, the prolonged hyperglycemia generates a breakdown of the BM, leading to local ischemia and tissue hypoxia. The latter induces an activation of hypoxia-inducible factors including VEGF, ultimately leading to an abnormal neovascularization of the choroid [16].

- Retinitis pigmentosa

Retinitis pigmentosa (RP) regroups several inherited retinal diseases with more than a hundred identified genes and more than 3000 reported mutations, leading to various pathological forms, and affecting 1 in 3000–5000 people worldwide [17–19]. RP can either be inherited as an autosomal-dominant (around 35% of cases), autosomal-recessive (about 55%), or X-linked (around 10%) disease, with symptoms appearing between the early childhood and adulthood [18]. The genetic mutations can affect the RPE, notably in the case of the bestrophinopathies, in which defects in pathways involved in the visual phototransduction cascade and ultimately in vision loss are observed. In many other cases, the genetic default will lead first to damage or death of the photoreceptors which will further trigger alterations in the RPE and thus in its barrier function causing a worthening of the pathology [20].

- Choroideremia

Choroideremia (CHM) is a X-linked recessive inherited disease caused by mutations in the *CHM* gene, encoding the Rab Escort Protein-1 (REP1) [21]. This rare disease is characterized by degeneration of RPE, photoreceptors and choroid layer, causing vision loss and blindness. However, the primary retinal cell type responsible for the onset of the degeneration is still unknown. There is currently no treatment for the choroideremia. Although gene therapy for the delivery of non-mutated *CHM* gene using adeno-associated virus has shown some promises [22], the clinical trial has been stopped.

- Gyrate atrophy

Gyrate atrophy is a rare recessive disease characterized by progressive loss of vision caused by chorio-retinal degeneration [23]. The disease is due by a deficiency of ornithine-aminotransferase (OAT) and 68 pathogenic mutations have been reported. Ornithine is a non-essential amino acid that plays an important role in the metabolism of urea. In patients with gyrate atrophy, the ornithine concentration in plasma, urinary, aqueous-humour and cerebrospinal fluid is ten to twenty times higher than in healthy subjects [24]. The oral administration of B6 vitamin (cofactor of ornithine aminotransferase) is able to decrease plasmatic ornithine concentration, and decelerate the disease progression in a small percentage of patients [25].

- Oculocutaneous albinism

Oculocutaneous albinism (OCA) is a group of inherited disorders affecting the melanin biosynthesis leading to a generalized reduction of the pigmentation in the hair, the skin and the eyes, and thus a disruption of the RPE pigmentation [26,27]. Eight different types of OCA are distinguished affecting different genes, with different levels of gravity. Notably, with a global prevalence of 1:40,000, OCA1 is the most severe form of the pathology, caused by a mutation of the gene encoding for

Tyrosinase (TYR) and leading to a complete disruption of the melanin biosynthesis [28]. More frequent in the African population with a prevalence of 1:3600–10,000 (vs. 36,000 for Europeans population), the OCA2 type is affecting the melanosome pH due to a mutation in the P Gene/OCA2 gene [28].

- Stargardt disease

First described in 1909 by Dr. K. Stargardt, the Stargardt disease (STGD1) is an autosomal recessive disease, caused by a mutation on the gene ABCA4 (ATP Binding Cassette Subfamily A Member 4) gene. Located in the POS, the protein encoded by the ABC4A gene is responsible for the transport of retinoids in the visual cycle. When the ABC4A protein is dysfunctional, insoluble retinoid derivatives accumulate in the POS, further phagocytosed by the RPE where they accumulate causing damage and ultimately cell degeneration [29,30]. With a prevalence of 1 in 8000–10 000, STGD1 is the most prevalent cause of inherited blindness in children, with an onset usually occurring in the two first decades of a life [31]. However, no efficient treatment is available to this day. Yet, several therapeutic strategies are currently investigated, from gene therapy to cellular therapy, as well as small molecule administration [29].

- Doyne honeycomb retinal dystrophy/Malattia Leventinese

Doyne honeycomb retinal dystrophy (DHRD) and Malattia Leventinese (ML) were first described in England in 1899 and in Switzerland in 1925, respectively. They were considered as distinct diseases until 1999 when it was shown that both conditions are caused by the same single autosomal R345W mutation in the fibulin-3 (or EGF-containing fibrillin-like extracellular matrix protein 1 (EFEMP1)) gene [32]. This mutation induces a misfolding and an abnormal accumulation of the protein in the RPE and between the RPE and the BM [33]. It is believed that this may create a physical barrier that could disturb the transport of other molecules between the RPE and the choroid, resulting in an accumulation of those molecules and the formation of drusen [34]. The first symptoms appear around the 30–40 years of age and there is to this day no efficient treatment. However, due to its many resemblances with AMD, the interest in the disease increased and AMD therapeutic strategies are investigated for DHRD/ML [35].

- Sorsby's fundus dystrophy

First described in 1949, Sorsby's fundus dystrophy (SFD) is an autosomal dominant monogenic disease with a prevalence around 1:220,000 [36]. With an onset between the 4th and 6th decade of life, the SFD is due to mutations on the tissue inhibitor of metalloproteinases-3 (TIMP3) gene. In healthy individuals, the TIMP3 protein is expressed by RPE and is involved in regulating the BM's thickness as well as inhibiting VEGF pathway and angiogenesis [36]. However, in its mutated form, the protein forms abnormal intermolecular disulphide bonds, leading to the formation of TIMP3 dimers which accumulate and form drusen-like deposits between the RPE and the BM. Further developments usually involve the apparition of a neovascularization, sub-retinal haemorrhage and retinal epithelial detachment, often leading to a misdiagnosis of AMD.

2.3. Consequences of the oBRB affecting diseases on the ocular immune privilege

As can be seen from the description of these pathologies, they all induce a disruption or even a breakdown of the RPE, caused by or leading to a loss of the photoreceptors. Both events ultimately lead to the perturbation of the ocular immune privilege [37]. Thanks to the two BRBs and the lack of lymphatic vessels, the retina is indeed an immune privileged tissue, where the immune cells differentiate into cells that suppress inflammation and promote immune tolerance, to preserve vision [38]. The RPE actively participate to this immune privilege notably by expressing immunosuppressive factors to suppress activation of $CD4^+$ and $CD8^+$ T cells and dendritic cells and to induce the apoptosis of monocytes and lymphocytes in order to prevent their accumulation and infiltration within the retina [5,38–41]. The RPE disruption, with a perturbation of its tight junctions, and the photoreceptor loss in the oBRB affecting diseases modify the immune environment of the retina. An increase of pro-inflammatory factors secretion, such as TNFα and VEGF, along with a decrease of anti-inflammatory factors have been observed [42,43]. These inflammatory changes affect the RPE, causing or enhancing its breakdown, further disrupting the immune environment [43,44]. In case of BRB disruption, the ocular antigens, normally sequestered due to lack of lymphatic drainage, can reach circulation causing T cells activation and their infiltration in the retina. Due to the disease-mediated absence of immune suppressive molecules, the immune cells can then elicit an inflammatory reaction against self-cells, which further increase the retinal degeneration [43]. Thus, several protective mechanisms are disrupted in these diseases, compromising the ocular immune privilege and leading to a worthening of the pathology.

3. Towards a more complex model of the oBRB

The mechanisms underlying these diseases are yet poorly understood and for most of them, no efficient treatment is available, especially for patients diagnosed in late stages and showing signs of retinal degeneration. To improve the knowledge on those diseases and address the lack of treatments, numerous oBRB models have been developed. These oBRB models present different degrees of complexity, notably in terms of the number of cell types included in the model and of the engineering of the material support. It should be noted that we will focus in this review on models that used human cell lines.

3.1. Models of the retinal pigment epithelium and the Bruch's membrane

A majority of the models focus on the RPE monolayer, with a support acting as the BM, and thus do not include the choroid. It is often considered that the most reliable RPE models, notably for drug permeation studies, rely on the use of explanted oBRB tissue sheets and a few studies directly used explanted human BM as a support for RPE culture. In the 1990's, human fetal RPE were harvested with the BM and grown *in vitro* as a sheet [45]. Designed for a cellular therapy against wet AMD, the graft however showed limitations with the development of cystoid-like macular edema in some patients. More recently, Moreira et al. studied the effect of BM aging on cellular behaviour by seeding RPE cells on BMs of human donors, either young (<46 years old) or old (>74 years old) [46], gathered as a full piece and decellularized. They further showed that the BM from old patients could be partially repaired by coating them with extracellular matrix (ECM) proteins to reconstitute a younger BM [46,47]. Instead of using the explanted BM as a full piece, Kim et al. developed a bioink from porcine BM that can be 3D printed to mimic the fibrous structure of the BM. Compared to a laminin coated plate, RPE cultured on the bioink demonstrated a higher expression of RPE markers, which can be due to both the composition and the topography of the printed scaffold [48]. Despite the biological advantages of using explanted tissues, the availability of donors and the access and isolation of the BM are particularly challenging. Thus, to cope with the limitation of ex-vivo tissue models, various support materials for RPE culture have been used throughout the last decades.

- Transwell PET insert

One of the most straightforward strategies consists in cultivating the RPE on a Transwell polyethylene terephthalate (PET) membrane to mimic the BM. Maugeri et al. and Doganlar et al. used this cell culture

support to model diabetic macular edema, by cultivating RPE cells on a Transwell under hyperglycaemic and hypoxia conditions. This model allowed them to analyze the beneficial or worthening effect of various molecules on the RPE such as the vasoactive intestinal peptide (VIP), the pituitary adenylate cyclase-activating polypeptide (PACAP), nicotine, melanin and caffeine (see section 4.2.2) [49–53].

To enhance cellular adhesion, the Transwell membrane is often coated with ECM proteins. For instance, to study drug permeation across the RPE, Mannermaa et al. developed an oBRB model by culturing RPE cells on a laminin coated Transwell membrane and showed that, despite a higher permeability, the cell model had similar transport trends than fresh bovine oBRB tissue [54]. Transwell membranes, coated with either Matrigel, fibronectin, gelatin, collagen, laminin or ECM from human placenta, were used for various *in vitro* applications, notably early drug screening, comparison of the drug permeability of multiples RPE cell lines [55,56], development of a standard protocol to cultivate RPE cells [57] and development of diseased models for oculocutaneous albinism [58] or choroideremia [21].

Besides *in-vitro* applications, several models used Transwell membranes as a scaffold for retinal tissue engineering, especially for cell therapy in AMD. Notably, Stanzel et al. coated the membrane with placenta ECM to cultivate RPE cells. The membrane was then implanted in the subretinal space of rabbits and non-human primates resulting in good cell survival and preservation of their polarization [59,60]. A similar study was conducted by Ilmarinen et al. who successfully implanted a monolayer of RPE cells cultured on a laminin coated Transwell membrane in the subretinal space of rabbits [61] and in Cynomolgus monkeys with a mechanically disrupted oBRB. In this study, the RPE cells kept their phenotype for up to a month post-transplantation [62]. PET membrane as a support for RPE implantation was even translated into clinics in a study by Da Cruz et al. After pre-clinicals trials conducted in a NIH III nude mice for the tumorigenicity study and in pigs for surgery feasibility, safety and biodistribution, they implanted RPE cells cultivated on a vitronectin coated membrane in 2 patients. After 1 year, the cells were still alive and functioning and the visual acuity of the patients improved (see section 4.3.3) [63].

Instead of directly implanting it, the culture insert has also been used as a temporary support for the formation of a RPE sheet, further detached and implanted without the PET membrane. To do so, the insert membrane is coated with a thin hydrogel layer that can be further dissolved to detach and gather the cell sheet from the Transwell. For instance, in a recent study by Soroushzadeh et al., the membrane was covered with an RGD (Arginylglycylaspartic acid)-functionalized alginate hydrogel, removed after RPE monolayer formation by application of sodium citrate and the cells sheet was successfully transplanted in the subretinal space of RCS (Royal College of Surgeons) rats [64]. Similarly, Kamao et al. used a collagen coated Transwell insert to form a monolayer of RPE cells, gathered by application of collagenase on the insert [65]. Pre-clinical trials were successfully conducted in diseased models of both rats and non-human primates and this system is currently under clinical trial [65–67]. This group most recently focused on the development RPE strips, acting as an intermediate strategy between cell injection and RPE sheet implantation [68]. Even if promising, the strips need further optimization, notably to avoid multilayering and to preserve RPE orientation during implantation.

Besides Transwell PET inserts, other commercially available membranes used to culture RPE are ultrathin equine collagen membrane from Resorba Medical GmbH [69] and ipCELLCULTURE synthetic polyimide membrane from It4ip [70,71]. For the latter, the study of multiple coatings such as laminin, laminin peptide, heparin sulphate, hyaluronic acid, collagen type I or IV, or commercially available ECM solutions (CELLStart™ from Gibco-Invitrogen, MaxGel™ from Sigma-Aldrich or HyStem-C™ from Glycosan Biosystems) revealed that the laminin was best suited to culture RPE cells [70].

- Custom membranes

As an alternative to commercially available supports, several groups developed their own membrane to culture RPE monolayers allowing them to control the physical, chemical, mechanical and biological properties of the material to better match tissue requirements.

Numerous studies have chosen to use synthetic materials, easily accessible and tailorable. One of the first studies developing a RPE synthetic implant was published in 1997 by Giordano et al. who investigated multiples well-known synthetic biodegradable polymers such as poly (L-lactic-*co*-glycolic acid) (PLGA) and poly (L-lactic acid) (PLLA). Even with a short-term culture and a poor characterization of the cells, this work paved the way by identifying potential materials for RPE replacement [72]. PLGA was characterized i*n vivo* more than two decades later by another group who implanted 10 μm thick PLGA membranes covered with a RPE monolayer in a healthy and a diseased rat model and in a pig model with RPE laser injury [73]. With no inflammatory response either in rats or in pigs, and a better integration and functionality of the RPE upon implantation compared with cell injection, the PLGA implant is currently under clinical trials (see section 4.3.3).

Following the steps of Giordano et al., various synthetic materials have been investigated for RPE transplantation and, as for Transwell membranes, a material functionalization was often required to enhance or even allow cellular adhesion. Poly (hydroxybutyrate-*co*-hydroxyvalerate) (PHBV8) films, polydimethylsiloxane (PDMS), and expanded polytetrafluoroethylene (ePTFE), all plasma treated, and poly-D-lysine coated methacrylate and methacrylamide hydrogel were showed to be suitable for the culture of RPE cells [74–78]. All of these studies synthesized their materials using the solvent casting technique, easy to implement and leading to smooth homogeneous membranes with usually a small porosity. A more complex geometry was developed by Lu et al. who selected Parylene-C as a material to design their membrane. They obtained an implant composed of a 0.3 μm thick smooth permeable membrane supported by a 6 μm thick mesh, all made with parylene-C and coated with either Matrigel for *in vitro* assays or with vitronectin for *in vivo* applications [79,80]. Covered with a monolayer of RPE cells, this implant called rCPCB-RPE1 has been evaluated in both rats and minipigs to assess the feasibility of implantation and therapeutic benefits against wet AMD and is currently under clinical trials (see section 4.3.3) [81–86].

Recently, the breath figure (BF) method has also been used to create thin membrane with a homogenous honeycomb-like porosity using polybutylene succinate (PBSu) [87]. The authors showed that membranes synthesized with the BF method favored RPE cell adhesion and production of extracellular matrix, compared to membranes generated by particle leaching technique (both membranes being coated with collagen IV and laminin). However, the study is still preliminary going solely up to day 5, with low cell characterization and absence of monolayer formation.

Even if the previous synthetic materials allowed cellular adhesion and proliferation, they differ from the BM in terms of topography. Indeed, the BM is mainly composed of collagen fibers and has thus a highly fibrous surface. To better mimic this characteristic, the electrospinning technique has been widely investigated using synthetic materials. Interestingly, it has been showed that the RPE cells cultured on electrospun membranes demonstrated a better morphology than ones cultured on smooth films, enhancing the importance of the material nano to micro-structure for cell maintenance [88,89]. The benefits of the electrospinning were further demonstrated by Liu et al. who studied the influence of the fibers diameters, ranging from 200 nm to 1000 nm, on RPE cells, seeded on electrospun membranes of PET or poly (L-lactide-*co*-ε-caprolactone) (PLCL) (see section 4.3.1) [90]. Since then, several studies have successfully developed electrospun grafts for retinal tissue engineering using various materials such as pectin-polyhydroxybutyrate [91] or polycaprolactone (PCL) modified

with integrin-binding peptides [92], enabling RPE monolayer formation with expression of classical markers.

Despite the numerous advantages of synthetic materials, notably in terms of access and processing, their functionalization is often limited and do not fully apprehend the complexity of a native tissue. Also, as previously mentioned, the use of oBRB explanted tissue is highly limited. However, one option to better model the BM is to use naturally sourced material from animal or human donors. In this optic, human amniotic membrane (hAM) has been investigated several times as a RPE culture support. Notably, an oBRB model for cell therapy based on a RPE monolayer on hAM was tested in rats and non-human primates [93,94] and is now in clinical trials (see section 4.3.3). More recently, RPE cells cultivated on hAM showed better cellular behaviour compared to Matrigel coated Transwell or culture plate [95]. To further improve the properties of the hAM, the latter was used as a powder and mixed with PCL to create an electrospun scaffold for cellular therapy in AMD or retinitis pigmentosa [96]. Optimal RPE behaviour was obtained on the membrane with 30% hAM powder.

Another human explanted tissue used for RPE culture is human anterior lens capsule, obtained after cataract surgery [74]. Composed

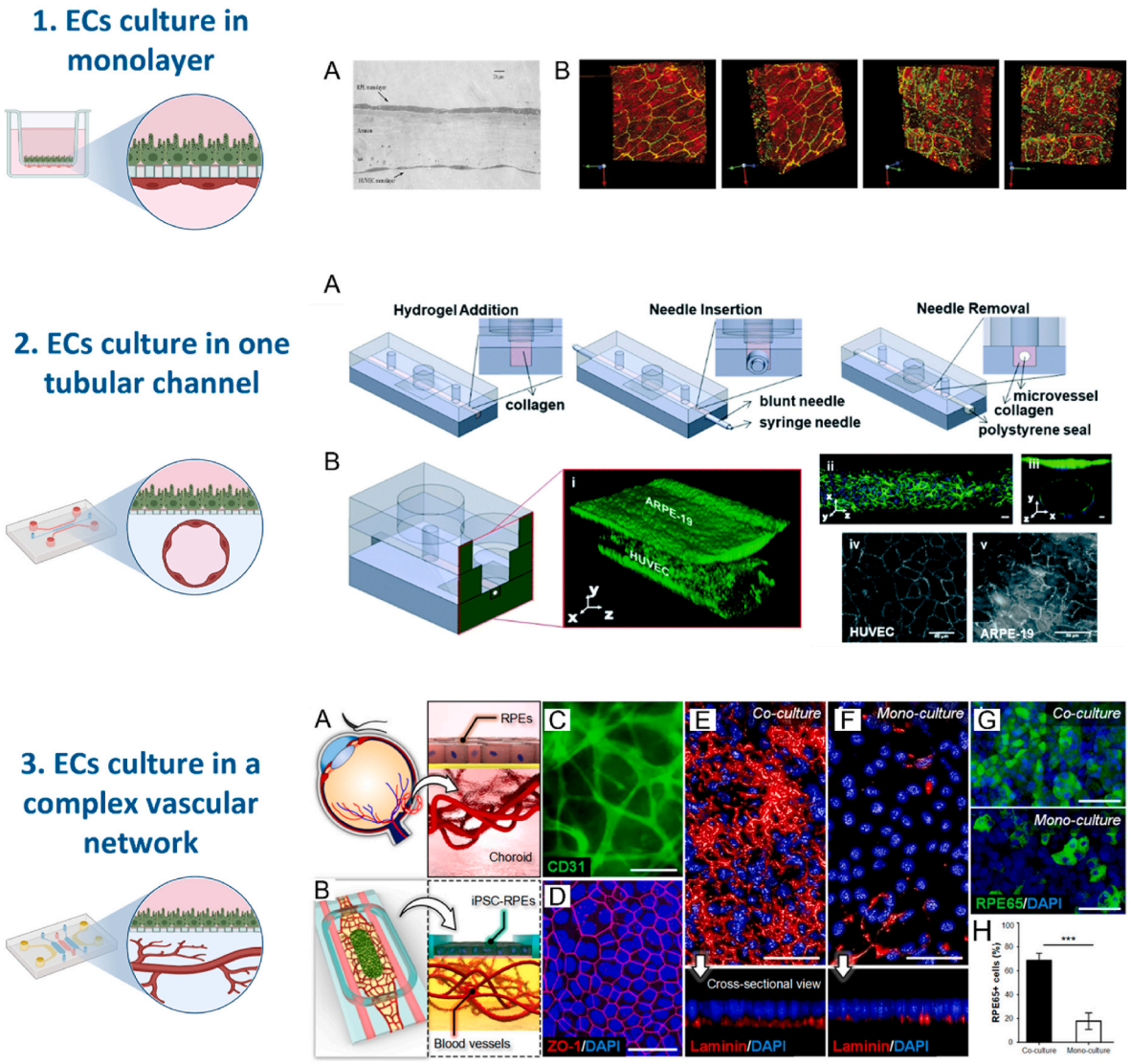

Fig. 2. From simple to complex oBRB co-culture models. 1/ ARPE-19 and HUVECs cultured on the two sides of a decellularized amniotic membrane. (A) Toluidine blue-stained trilayer showing monolayers of the RPE (above) and the HUVECs (below). (B) Confocal micrographs of optical sections of the trilayer tilted around its axis, with images have been tilted at varying angles [starting with the RPE surface (left side) to the HUVEC surface (right side)] using Velocity software and with immunostaining for ZO-1 (green) and occludin (red). Adapted from Hamilton et al. [101] with permission of John Wiley and Sons. **2/ PDMS-based chip device for the 3D co-culture of an ARPE-19 monolayer above a microvessel cultured with HUVECs.** (A) Schematic representation of the patterning of a collagen I hydrogel using the subtractive method to create the microvessel. (B) (i) 3D construction of confocal image of the co-culture system stained for nuclei and actin filaments, revealing (ii) an equal distribution of HUVECs along the microchannel as well as (iii) the ARPE-19 monolayer located above the microvessel. These cells were positive for their respective cell–cell adhesion markers: (iv) VE-cadherin for HUVEC and (v) ZO-1 for ARPE-19. Scale bars: 50 μm. Adapted with permission (Creative Commons Attribution 3.0 Unported Licence) from Arik et al. [108] **3/ Microengineered model of the oBRB with complex vascularization.** (A) Schematic view of the oBRB and (B) its modelization by culturing human iPSC-derived RPEs on the surface of a hydrogel construct containing a network of blood vessels. (C) Microvessels at day 14 constructed by primary human retinal microvascular endothelial in co-culture with choroidal fibroblasts embedded in a fibrin scaffold. (D) Well-defined intercellular tight junctions (ZO-1) in the iPSC-RPE monolayer after 14 days of culture. The beneficial effects of the co-culture of RPE cells with ECs, compared to a RPE monoculture are observed in (E–F) the production of basement membrane proteins by the RPE on the basal side after 14 days and in (G–H) the increased expression of RPE-specific markers such as RPE65 after 14 days. Scale bars are 50 μm ***$P < 0.001$ ($n = 3$). Adapted with permission from Paek et al. [111]. Copyright from American Chemical Society. Figure created with *BioRender.com*.

mostly of type IV collagen and laminin, as the native BM, the lens capsule is a good candidate for RPE cell therapy and human adult RPE cultivated on this substrate displayed typical RPE behaviour. However, as for all human derived material, its availability remains an important limitation.

To overcome the need for human donors, *Bombyx mori* silk fibroin (BMSF) has been investigated in the last ten years. A group developed 3 μm thick membranes using BMSF coated with commercial ECM from human placenta to cultivate RPE cells which displayed a stronger expression of RPE markers compared to a culture on Transwell [97]. Later on, the same membrane coated with collagen type I proved to be an adequate substrate to culture RPE cells for up to 3 months [98]. This membrane was further optimized by addition of polyethylene glycol (PEG) and horseradish peroxidase to improve its permeability and mechanical properties for surgical handling respectively and was successfully implanted in the subretinal space or in the retinal parenchyma of RCS rats with retinal dystrophy [99].

3.2. Models recapitulating the retinal pigment epithelium, the Bruch's membrane and the choroid

In recent years, advances in the field of microfabrication and 3D cell culture have led to the emergence of studies in which RPE cells are co-cultured with endothelial cells (ECs) to also recapitulate the choroidal compartment of the oBRB. As for models in which only the epithelium was considered, the complexity of the proposed supports has increased with time to better mimic the tissue.

- Transwell PET insert

The first reported study combining the culture of RPE and ECs was published in 2003 by Hartnett et al. To study the effect of ECs on the barrier function of RPE monolayer, bovine cells were cultured in a Transwell culture system following different strategies to evaluate contact and non-contact co-culture. This study was pioneer but presented numerous limitations, including the animal origin of cells and the culture of ECs in monolayers which could explain in part the negative outcomes, notably the reduction of the RPE barrier function in the presence of ECs [100]. This result contrasts with further studies also using monolayers of ECs. For instance, minusheet carriers have been used to co-culture RPE cells and HUVECs on each side of the amniotic membrane (Fig. 2.1) [101]. In the presence of RPE cells, ECs became fenestrated, a phenomenon characteristic of the oBRB and that was not observed in co-culture with corneal epithelial cells. In addition, the presence of ECs was enhancing the polarization of the epithelium monolayer. Similarly, after 4 weeks of culture on opposite sides of a Transwell membrane, HUVECs improved maturation and function of RPE cells with an increase of antiangiogenic markers that are known to contribute to the maintenance of retinal homeostasis [102]. The beneficial effect of the co-culture with ECs to regulate oBRB was confirmed more recently with a similar setup with RPE cells seeded on Transwell inserts and ECs forming a monolayer on the bottom of the well plate [103]. Results demonstrated that the remodelling of the RPE basement membrane with enhanced tight junctions and barrier functions is mediated by the secretion of angiocrine factors by mature choroid ECs.

Co-culture techniques using Transwell systems also allow delving into the mechanisms involved in retinal diseases, by placing the model under pathological cues. This is the case of the work by Kumar et al. set up to elucidate the interaction mechanisms between human retinal progenitor cells and ECs that modulate neovascularization, at the origin of wet AMD (see section 4.2.2) [104].

- Custom membrane

Instead of using commercial Transwell membranes, Calejo et al. developed their own membrane in polylactide (PLA), coated with collagen [105]. To control the membrane porosity, they used the breath figure method, resulting in a homogeneous honeycomb porous structure. They cultivated RPE cells with two different types of ECs, in a monolayer on the opposite side of the membranes. If this set-up enabled the analysis of some interactions between the cells, notably by studying the cell number, the study lacks proper characterization of the cells to properly conclude on the beneficial effect of co-culture.

- oBRB on chip

Since 2017, oBRB on chip models that incorporate epithelial and ECs have emerged. These microfluidic devices allow building up miniaturized tissues in which the interface between the epithelium and the endothelium is reproduced under dynamic conditions. The most classical approach consists in a device with two channels separated by a membrane with two monolayers of cells, RPE cells and HUVECs, on each side of it [106]. By using this model, the authors attempted to monitor choroidal angiogenesis under hypoxia and in the presence of different glucose levels and demonstrated that, in all conditions, HUVECs invaded and disrupted the epithelial layer. However, it is difficult to establish conclusions based on these results, since relevant aspects of the oBRB were missing, including the level of maturation of the epithelial cell monolayer at the beginning of the study, the characteristics of the HUVECs layer and the choice of the applied flow. In a later work by the same team, the microfluidic device was upgraded to demonstrate its versatility with the addition of two channels for fibroblasts seeding, as support cells, and the incorporation of platinum electrodes for *in situ* TEER (transepithelial electrical resistance) measurements [107]. Unfortunately, none of the key biological issues highlighted above were addressed in their study.

Following the technological evolution in the field of microfluidic chips, Arik et al. used a mask to build a PDMS chip with a patterned square-channel that was filled with a fibroblast-loaded pre-patterned hydrogel moulded around a needle to obtain a rounded channel where HUVECs cells were seeded. A polyester membrane separated this vascular compartment from the RPE cells monolayer (Fig. 2.2) [108]. Despite the large dimensions of the channel (0.9 mm) and the lack of a dense vascular network, this device succeeded to mimic oxidative stress resulting in a decrease of the barrier integrity. Several years ago, the use of masks to pattern a fractal tree on photo-crosslinked gels was already proposed but that system was poorly studied focusing only on cell spreading and proliferation [109].

- Hydrogels

The possibility to incorporate hydrogels into the microfluidic chips is still at its infancy, particularly when we want to reproduce complex patterns, but it already offers the possibility to prepare more physiologically relevant dynamic models of the oBRB. A 3D on chip co-culture model with RPE cells seeded on a blank fibrin hydrogel on top of a fibrin gel loaded with HUVECs was used to build an *in vitro* disease model [110]. In this device, pathological angiogenesis under VEGF exposure could be reverted with an antiangiogenic drug (Bevacizumab) used to treat wet-AMD (see section 4.2.2). Fibrin gel was also used to engineer a versatile hybrid platform to engineer several types of perfusable 3D microvascular beds, including a model of oBRB constituted by a monolayer of RPE cells, primary human retinal microvascular ECs and choroidal fibroblasts (Fig. 2.3) [111]. By comparing the monoculture of iPSC-RPEs with the co-culture with the ECs, an increase of laminin deposition in the basement membrane was observed, as well as greater pigmentation of RPEs with an increase of the number of melanosomes, and increased expression of RPE65 specific marker.

An important novelty of the latest models of oBRB is the incorporation of support cells that has contributed to establish more mature models for long-term culture studies. In this context, Manian et al. developed a platform to investigate RPE-choroid biology, macular

degeneration pathophysiology, and to find new therapies [112]. A hydrogel specifically designed to enable matrix remodelling (more details are provided in section 4.2.1) incorporated patient derived iPSCs differentiated into RPE, ECs and mesenchymal stem cells (MSC). Noteworthy, the presence of the MSCs was key to prolong the culture from 2 weeks to 2 months. They could reveal the role of RPE and MSC factors for the development of the choriocapillaris complex, as well as the contribution of other local and systemic factors in macular degeneration. With the same purposes, Song et al. recently combined in a very elegant system, iPSCs differentiated into RPEs and ECs, primary pericytes and primary fibroblasts [113]. This work demonstrated the importance of the combination of those four cell types to promote angiogenesis and induce a choroidal phenotype, leading to the formation of long-term capillaries of 20–50 μm lumen size. Interestingly, using cells derived from AMD patients, this model of oBRB replicated changes in the BM and in the choriocapillaris as observed in macular degeneration (see section 4.2.2).

4. Major considerations about the oBRB models

4.1. Cell types for oBRB models

4.1.1. Retinal pigment epithelial cells (RPE cells)

The *in vitro* culture of human RPE (hRPE) cells started in the 1970's, using explanted RPE cells following the method of Mannagh et al. [114]. With the elaboration of RPE cell lines, the access to RPE cells became easier and research on RPE increased significantly. Over the years, numerous RPE cell types were studied and used in oBRB models, either grown from established cells lines, explanted from living or dead, adult or fetal donors or generated from stem cells. We will discuss here each cell type for their proven suitability for oBRB modelling taking into consideration the material support used and its functionalization. For further discussion about culture protocols specifications such as cell-harvesting method, media composition, seeding densities or passaging rates the reader can refer to previous reviews covering these specific subjects [115]. Moreover, we will not discuss here studies that developed injections of RPE suspension, without support, to treat various retinopathies.

4.1.1.1. Cell lines

4.1.1.1.1. ARPE-19. One of the most used human RPE cell line is the ARPE-19, a well-established but non-immortalized line. It emerged spontaneously from primary RPE cells isolated 2h after the death of a 19-year-old male human donor [116] and is now commercially available. Numerous oBRB models have used ARPE-19 in monoculture [46,48–54,69,76,77,79,91,92,96,97,117,118] and co-cultured with ECs [101,102,106–108,110] to generate a RPE monolayer for drug permeation studies [54,117], for tissue [101,102,106,107] and disease modelling [46,49–51,53,108,110], for material suitability analysis for RPE culture [48,118] or for graft development against various retinal diseases, mostly AMD [69,76,77,79,91,92,96,97,118]. Several material and functionalization protocols were developed for ARPE-19 culture (See section 4.2.1 and 4.3.1 and Tables 1 and 3). Overall, each method enabled cellular attachment and proliferation, with the formation of a confluent RPE monolayer, with cells displaying the typical cobblestone RPE morphology. ARPE-19 cells form a monolayer in a week [69,77] depending on the seeding density. However, in some studies, the cellular proliferation continued after formation of the confluent monolayer leading to overgrowth and multilayering [54,77]. This can be overcome by tailoring the media composition, for instance, by adding retinoic acid to a 10 μM concentration [77]. ARPE-19 express classical RPE markers such as ZO-1, RPE65, VMD2, CRALBP, MITF, TRP-1, tyrosinase, VEGF, Ezrin and PEDF, with expression levels being impacted according to the substrate on which the cells are seeded [48]. Moreover, in multiple studies, ARPE-19 cells have been proven to be able of phagocytosis, a key property of RPE cells [46,48,69,76,77,97,101,102]. Thumann et al. demonstrated that phagocytosis of porcine rod outer segments was more efficient when ARPE-19 cells were seeded on a collagen type I membrane compared to plastic [69].

Nonetheless, the ARPE-19 cell line presents some morphological and developmental differences from natural RPE monolayers. First, they lack melanin-induced pigmentation, a major factor in ocular pharmacokinetics, affecting both drug distribution and retention in ocular tissues [119]. By increasing the cultivation time, Shadforth et al. observed a partial pigmentation, of 25–50% of the cells after 12 weeks in culture [97]. To address this limitation, a team established a new artificially pigmented ARPE-19 cells called ARPE-19mel [119] by isolating melanosomes from porcine RPE and incubating them with ARPE-19. The melanosomes were spontaneously phagocytosed by and integrated into the cells. The resulting pigmentation was retained during the entire cell cultivation and its intensity could be adapted by adjusting the concentration of administrated melanosomes.

Secondly, if the presence of tight junctions between the epithelial cells was assessed with ZO-1 staining [77], the original derivers of the cell line reported low transepithelial resistance (TER) values for the ARPE-19 sublines, with values reaching a maximum of 50–100 $\Omega \bullet cm^2$ [116]. Since the TER in the native human RPE-choroid tissue has been measured around 150 $\Omega \bullet cm^2$ [120], this shows that an ARPE-19 monolayer is less effective as a barrier than the native tissue, with weaker junctions and/or lower confluence. Subsequent studies using ARPE-19 made similar observations, with values as low as 40 $\Omega \bullet cm^2$ with ARPE-19 cultivated on uncoated Transwell membranes [49–52] or even 30 $\Omega \bullet cm^2$ when cultivated on BM bioink [48]. Strategies to increase the ARPE-19 TER value have been developed. For instance, Mannermaa et al. studied eight different culture media composition and obtained TER values ranging from 80 to 160 $\Omega \bullet cm^2$, the latter being obtained by addition in the basic medium of 1% FBS, basic fibroblast growth factor (10 ng/mL), sodium pyruvate (1 mM) and taurine (10 mM) [54]. Shadforth et al. obtained an even higher value of TER of 250–300 $\Omega\ cm^2$ by cultivating the ARPE-19 on a *Bombyx mori* silk fibroin membrane coated with human placenta ECM [97]. These lower TER values in ARPE-19, synonym of less effective barrier functions, can impact the permeability of the tissue. Indeed, Mannermaa et al. showed that the permeability of an ARPE-19 monolayer on laminin coated Transwell is higher than the one of fresh bovine tissue, from basal to apical and from apical to basal. If the two models showed similar transport trends and qualities, they are not similar quantitatively which would notably affect drug testing results [54]. However, as they showed for the TER, the permeability can also be tailored by the media composition, as for instance by addition of 25 nM Tretinoin (ATRA) [54].

Some studies have also demonstrated limits in the polarization of the ARPE-19. For instance, when cultured on silk fibroin membranes, the ARPE-19 did not secreted VEGF and PEDF in a polarized way, with similar concentrations measured on the basal and apical sides [97]. One of the most striking studies analysing the relevance of ARPE-19 to mimic natural RPE is the one by Kamao et al. who conducted a micro-assay using more than 57,000 probes and analysed 154 genes to characterize hiPSC-RPE in comparison with ARPE-19, hRPE, and fibroblasts. They obtain a phylogenetic tree where the ARPE-19 were actually closer to fibroblasts than hRPE, questioning the use of ARPE-19 to model hRPE [65].

4.1.1.1.2. D407. Another cell line, less studied for oBRB modelling, is the D407 cell line. As for the ARPE-19 line, the D407 emerged spontaneously from primary RPE which were isolated 12 h after the death of a 12-year-old male human donor [121]. The cells were maintained in culture for over 200 passages while keeping characteristic markers of the RPE such as the epithelial morphology and the formation of a hexagonal cobblestone layer with tight junctions [121]. Tezcaner et al. used the D407 line to study the potential application of PHBV8 membranes modified by oxygen plasma treatment as an oBRB graft against retinal

Table 1
In vitro modelling of the outer blood-retina barrier.

	Application	RPE cell type	EC type	Model design	Relevant outcomes (+) and limits of the study (−)	Ref#
Healthy oBRB models	*In vitro* study of drug permeability across RPE monolayer	ARPE-19	None	Laminin coated Transwell	+ Importance of molecular size and lipophilicity on the drug permeability - Higher monolayer permeability than explanted bovine oBRB: weaker barrier junctions and underestimation of the cellular active transport	[54]
		hfRPE and hESC-RPE	None	Human ECM or laminin coated Transwell	+ Identification of 25 genes to assess the barrier properties of the RPE + Impact of the culture medium on the barrier function	[56]
		ARPE-19	None	Ammonia plasma treated ePTFE culture insert	+ Computational model to predict drug transport across the oBRB - Choice of the ARPE-19 line known for having weaker barrier function	[117]
	Effect of photodynamic therapy (PDT) on the RPE	Primary adult RPE	None	Semipermeable polycarbonate membrane	+ Addition of verteporfin with non-thermal laser, as used in PDT, induced a breakdown of the oBRB (absent without verteporfin) - Low characterization of cells	[123]
	Study of RPE-choroid interactions	ARPE-19	HUVECs	Monolayers on each side of amniotic membrane	+ HUVECs become fenestrated when co-cultured with ARPE-19 (and not with corneal epithelial cells) - 2D culture of the ECs and effect of dynamic flow not studied	[101]
		D407 RPE	HUVECs	Electrospun SF membrane for RPE, on a hyaluronic acid gel patterned with a tree-like EC structure	- Low ECs coverage of the tree network and aberrant phenotype of the RPE in co-culture - No possibility of inducing flow in the ECs network	[109]
	Study of ECs influence on RPE phenotype and ECM production	ARPE-19	HUVECs	Monolayers on each side of a Transwell, with laminin coating for RPE cells and gelatin coating for ECs	+ ECs improve maturation and function of the RPE cells + Increase of anti-angiogenic markers levels in co-culture	[102]
		hfRPE	HUVECs	Transwell for RPE, with ECs at the bottom of the plate well	+ Mature choroidal cells contribute to the remodelling of the RPE basement membrane and improve barrier function	[103]
		hiPSC-RPE	hiPSC-ECs, HUVECs, HRMVECs	Monolayers on each side of a polylactide collagen coated membrane	+ Optimization of the membrane porosity to avoid ECs migration + Comparison of the interaction of hiPSC-RPE with different EC types - Low characterization of the cells	[105]
	oBRB perfusable platform for tissue modelling and drug testing	ARPE-19	HUVECs	Microfluidic chip: Polyester membrane, for RPE culture, on top of a collagen I hydrogel with a microchannel for ECs	+ Addition of human lung fibroblasts to support vessel formation - Vessel diameter significantly larger than the choroid vasculature	[108]
		hiPSC-RPE	HRMVEC	Microfluidic chip: RPE seeded on top of a fibrin hydrogel encapsulating the ECs	+ Perfusable 3D microvessel network supported by human lung fibroblasts + Increased RPE markers expression, pigmentation and basement membrane proteins production in co-culture	[111]
Diseased oBRB models	AMD: Effect of BM aging on RPE behaviour	ARPE-19	None	Bruch's membrane from human young (<46 yo) donors or old (>74 yo) donors, further coated with ECM protein to see repair effect	+ Aged BM decreases the phagocytosis ability of the RPE recapitulating disease phenotype + Coating the altered BM with ECM proteins increases survival, proliferation, adhesion and phagocytosis of the RPE cells	[46,47]
		hiPSC-RPE from patients	None	ECM produced by ARPE-19 and altered with nitrite (to mimic aged BM)	+ Gene expression is altered in cells derived from AMD patients + Nitrite modification of the ECM reduces attachment and viability, especially for AMD RPE cells	[140]
	AMD (dry): effect of inflammation and study of nicotinamide as potential treatment	hiPSC-RPE from patients or controls	None	Culture plate	+ Higher levels of drusen-related proteins and increase of complement and inflammatory factors in diseased RPE + Nicotinamide improves disease-related phenotypes: potential therapeutic strategy for AMD treatment	[129]
	AMD: oBRB AMD platform to study disease mechanism and therapeutics	hiPSC-RPE	hiPSC-ECs	Microfluidic chip: Electrospun PLGA membrane for RPE on top of bioprinted gelatin-based hydrogel encapsulating the ECs, with pericytes and fibroblasts	+ Pericytes and fibroblasts help the formation of the vascular network + Model of dry AMD mimics drusen formation, capillary degeneration and loss of barrier function + Two strategies to model wet AMD (gene- and drug-based) lead to capillaries	[113]

(*continued on next page*)

Table 1 (*continued*)

Application	RPE cell type	EC type	Model design	Relevant outcomes (+) and limits of the study (−)	Ref#
				hyperproliferation and RPE monolayer disruption	
	ARPE-19	HUVECs	Microfluidic chip: RPE seeded on top of a fibrin hydrogel encapsulating the ECs	+ Operational system within 4 days + Hypoxic conditions to mimic wet AMD inducing vascularization upregulation	[149]
AMD (wet): study of choroidal neovascularization	ARPE-19	HUVECs	Microfluidic chip: RPE seeded on a blank fibrin hydrogel, placed on top of another fibrin hydrogel incorporating the ECs (supported by fibroblasts)	+ Perfusable vascular network + Model of wet AMD: VEGF treatment promotes angiogenesis - Model requires a 300 μm thick gel between RPE and choroid to avoid vessel regression	[110]
	ARPE-19	HUVECs	Microfluidic chip: porous fibronectin coated PDMS membrane, with RPE on one side and ECs on the other	- ECs in a monolayer and poor characterization of the effect of continuous flow - Poor characterization of the RPE - Inconclusive effects of hypoxia and glucose increase	[106, 107]
ADRD; DHRD and SFD: Study of drusen formation and ECM alteration mechanisms	hiPSC-RPE from patients and control	None	Culture plates or Transwell	+ Presence of drusen-like sub-basal deposits after 90 days, rich in proteins and lipids, and accumulation of collagen IV in the ECM + Earlier onset of DHRD pathophysiology compared with SFD with differences in ECM and drusen composition	[147]
Choroideremia: study of disease pathogenesis	hiPSC-RPE from patients	None	Matrigel coated plates or fibronectin coated Transwell	+ Complete characterization of the RPE and the mutation effects (no expression of REP1) + Characterization of the disease effects on the Rab proteins and on phagocytosis by RPE	[21]
DME: effect of different molecules on the RPE	ARPE-19	None	Transwell; under hyperglycemic and hypoxic environment	+ Pituitary adenylate cyclase-activating polypeptide (PACAP); Vasoactive intestinal peptide (VIP) and caffeine counter the effects of hyperglycemia and hypoxia while nicotine worthen them	[49–52]
	ARPE-19	None	Transwell; under hyperglycemic and hypoxic environment	+ Melatonin improves TEER, reduces RPE permeability and protects against mitochondrial dysfunction - Low characterization of the cells, besides mitochondrial function	[53]
Gyrate atrophy: use of hiPSC-RPE to model the disease	hESC-RPE and hiPSC-RPE	None	Culture plates	+ hiPSC-RPE recapitulates the lack of OAT activity of the disease + Highlights vitamin B6 as potential treatment, with the optimal concentration of 600 μM	[137]
OCA: study of RPE pigmentation	hiPSCs-RPE from OCA1A and OCA2 patients or controls	None	Transwell	+ No pigmentation observed in OCA1A, with no mature melanosomes whereas OCA2 developed a small pigmentation with time (over 6 months), with only 32% of mature melanosomes: enhance the importance of the TYR gene for melanosomes maturation	[58]
SFD: platform to study disease mechanism and therapeutics	hiPSC-RPE from patients or controls	hiPSC-ECs from patients or controls	RPE seeded on top of a PEG hydrogel encapsulating the ECs	+ RPE secreted factors necessary for the formation of EC fenestrations + Choroidal neovascularization and capillaries atrophy can be initiated solely by RPE factors alterations, without previous drusen formation + Identification of 2 potential therapeutic targets: FGF-2 and MMPs - Lack of material characterization	[112]

Abbreviations: ADRD: autosomal dominant radial drusen; AMD: age-related macular degeneration; DHRD: Doyne honeycomb retinal dystrophy; DME: diabetic macular edema; OCA: Oculocutaneous albinism; SFD: Sorsby's fundus dystrophy; PDMS: polydimethylsiloxane; PEG: polyethylene glycol; PLGA: poly(DL-lactic-*co*-glycolic acid); ePTFE: expanded polytetrafluoroethylene; SF: silk fibroin, TER: transepithelial resistance.

disorders such as diabetic retinopathy, RP or AMD [75]. Thanks to the plasma treatment, the cells were able to adhere, with apparition of pseudopods revealing the onset of spreading after 8 h, and ultimately formed an organized monolayer in 7 days. More recently, D407 cell line was co-cultured in a contactless setting with HUVECs to build an oBRB on a chip [109]. The epithelial cells were cultured on top of an electrospun porous fibrin membrane that was placed in Transwell holders and introduced in a well containing methacrylate hyaluronic acid hydrogel seeded with HUVECs. In the presence of HUVECs, D407 cells lost their hexagonal morphology with visible cell extensions formed after 14 days that increased with time leading to a majority of spindle-like cells at day 21.

As far as we know, the D407 cell line is not commercially available, reducing its use, and was supplied as a gift in all studies. In addition, the marginal use of D407 cell line can also be due to its numerous drawbacks [121]. First, even if the cells are able to form a monolayer, they lack a

Table 2
Material characterization of the oBRB models for cellular therapy.

Material	Functionalization	Thickness	Topography	Wettability - Water contact angle	Mechanical properties	Additional characterization	Ref#
Collagen type I	None	7 μm	Smooth	80°	NR	NR	[69]
hAM + PCL	None	NR	Fibrous (electrospinning) with AFD of 200–300 nm	119 ° for PCL alone and 92° with hAM	Young's modulus (Tensile testing): 17,3 MPa for PCL alone and 40 MPa with hAM	Porosity: btw 85 and 90%	[96]
Bombyx mori SF + PEG + HRP	None	Btw 5–30 μm	Smooth	NR	Young's modulus (Tensile testing): 10–25 MPa	Permeability: btw 10^{-8} and $2*10^{-8}$ cm s^{-1}	[99]
Parylene-C (rCPCB-RPE1 implant)	*In vitro*: Plasma treatment or Matrigel *In vivo*: vitronectin	0,3 μm thick membrane on 6 μm thick mesh	Smooth	NR	NR	Diffusion coefficient btw 10^{-10} and 10^{-13} cm^2 s^{-1} for molecule btw 4 and 250 kDa	[79,80]
PBSu	Laminin 521 and Collagen IV	Around 20 μm	Honeycomb porosity Mean roughness (AFM): btw 150 and 660 μm	Btw 52 and 79°	NR	Pore diameter btw 1 and 3 μm	[87]
PCL	Integrin-binding peptides (iBPs)	2,16 μm	Fibrous (electrospinning) with AFD around 350 nm	92,4° for PCL and 20,2° for PCL + iBPs	NR	NR	[92]
Pectin-PHB	None	200 μm	Fibrous (electrospinning) with AFD btw 336 and 500 nm (Pectin/PHB ratio)	Btw 88 and 124° (Pectin/PHB ratio)	Young's modulus (Tensile testing): btw 0,08 and 0,23 GPa (Pectin/PHB ratio)	NR	[91]
PET	None	1–2 μm	Fibrous (electrospinning) with 200; 500 or 1000 nm fiber diameter	NR	NR	Average pore size: btw 0,23 μm^2 and 3,75 μm^2	[90]
PHBV8	Oxygen plasma treatment	5–10 μm	Smooth Mean roughness (AFM): 82,03 nm	58,3°	NR	NR	[75]
PI	Laminin	24 or 7,6 μm	Smooth Mean roughness (AFM): 82,03 nm	Around 50°	Tensile strength: 139 MPa	Pore diameter: 1 μm Porosity: $2,2*10^7$ pores/cm^2	[70,71]
PLGA	None	14 μm	Smooth (solvent casting) or fibrous (electrospinning) with AFD of 331 nm	NR	Young's modulus (tensile testing): 217,9 MPa for smooth and 131,9 MPa for fibrous material	NR	[88]
PLGA or PLLA	None	Between 20 and 36 μm	Smooth	NR	Loss moduli (Dynamic mechanical analyser): in the range of 500 MPa-50 GPa	NR	[72,170]
PLGA; PLLA or PLDLA or PCL	Laminin	Around 10 μm	Fibrous (electrospinning) with AFD below 70 nm and surface roughness (AFM): around 260 nm	NR	Young's modulus (AFM): 16 MPa for PCL; 25 MPa for PLGA; 31 MPa for PLDLA and 48 MPa for PLLA	Porosity: around 50%	[89]
ePTFE	Ammonia plasma treatment (PT) or *n*-heptylamine coating (nHA)	Around 100 μm	Fibrous with AFD btw 100–300 nm	133° for ePTFE, 68,5° for PT-ePTFE, 123,5° for nHA-ePTFE	Mean elastic modulus (AFM): 1–2 GPa	NR	[76,78]

Abbreviations: AFD: Average fiber diameter; Btw: Between; NR: Not reported; hAM: human amniotic membrane; HRP: horseradish peroxidase; PBSu: polybutylene succinate; PCL: Polycaprolactone; PEG: polyethylene glycol; PET: polyethylene terephthalate; PHB: polyhydroxybutyrate; PHBV8: Poly(hydroxybutyrate-*co*-hydroxyvalerate); PI: Polyimide; PLDLA: Poly(D,L-lactic acid); PLGA: poly(L-lactic-*co*-glycolic acid); PLLA: poly(L-lactic acid); ePTFE: expanded polytetrafluoroethylene; SF: silk fibroin.

complete polarization with notably short microvilli on the apical side and a loss of cytoskeletal polarization. Moreover, the loss some enzymatic activities such as lecithin retinol acyl transferase and retinoid isomerase compared to native RPE has been also demonstrated. Additionally, as for ARPE-19, the D407 cells fail to produce melanin. Thus, the melanin from the original cells is divided among the daughter cells without additional production, resulting in a complete loss of pigmentation over time.

4.1.1.2. Explanted cells - hRPE. Before the establishment of cell lines or the differentiation of stem cells, the only possible solution to obtain RPE cells was to directly harvest them from retinal tissue of living or recently deceased donors. We will focus here on human tissues and both human adult (haRPE) and fetal (hfRPE) sources will be analysed for their relevance for oBRB modelling. For harvesting methods and culture protocols discussion, the reader can refer to the review by Fronk and Vargis [115].

4.1.1.2.1. Human fetal RPE cells. Harvesting and culture of human fetal RPE (hfRPE) cells date back to the 1990's [45,72,122] and have been used in oBRB modelling in several studies ever since [57,59,90,103]. The hfRPE were harvested from fetuses between 10 and 20 weeks of gestation and were cultivated on various cell supports: Transwell inserts with various coatings (collagen, laminin, fibronectin, gelatin and human placenta ECM, the latter presenting the best results) [57], Transwell inserts with Matrigel [103], and membranes made out of PLGA, PLLA [72], PET [59,90] or PLCL [90]. Cells were able to adhere and proliferate on these substrates showing the typical cuboidal shape of RPE cells. It should be noted that the nature of the material and notably

Table 3
oBRB implants developed for RPE cellular therapy.

	Material	Cell type	In-vivo and clinical translation	Targeted disease	Outcomes and limits	Ref#
Natural materials	hAM (decellularized)	hESC-RPE	1) Nude rats 2) RCS rats 3) Immunosuppressed NHP	RP and dry AMD	+ Expression of typical RPE markers both *in vitro* and *in vivo* + Development of a GMP-compliant carrier to implant the graft + No teratoma formation + Improved visual acuity and increased photoreceptor survival *in vivo* - Immunogenicity of the graft and need for immunosuppression, the transplantation altering the oBRB	[93,94]
	hAM (decellularized))	hiPSC-RPE	New Zealand white albino rabbits	/	+ No modification of the hAM upon decellularization + All RPE marker expressions higher on hAM compared to Matrigel coated plate - Short term analysis *in vivo* (7 days)	[95]
	Bombyx mori SF + Human placenta ECM or collagen I	ARPE-19 or hiPSC-RPE	None	AMD	+ Phenotype closer to the native RPE with hiPSC-RPE than with ARPE-19 - No real benefits of the developed membrane compared to laminin coated Transwell	[97,98]
	Collagen type I	ARPE-19	Rabbits	AMD	+ Excellent biocompatibility of the membrane and 3-month stability at least in media - Poor characterization of cellular behaviour and phenotype - Use of the ARPE-19 cell line, unsuitable for implantation	[69]
Hybrid materials	hAM + PCL	ARPE-19	None	AMD or RP	+ Improved material properties by addition of hAM in the PCL + Optimal cellular phenotype with 30% hAM - Use of the ARPE-19 cell line, unsuitable for implantation	[96]
	Bombyx mori SF + PEG + HRP	hESC-derived RPE	RCS rats: acellular samples only	AMD	+ Increased permeability with PEG and reinforced cross-linking with HRP: membrane easier to handle and transplant + Increase of the growth factor expression after material modification - Lack of *in vivo* cellularized implantation to study graft efficiency	[99]
	Bruch's membrane (Porcine) and PCL	ARPE-19	Rats: acellular samples only	/	+ Improved ARPE-19 phenotype on the bioink vs. laminin coated Transwell + Suitable material properties for implantation - Use of the ARPE-19 cell line, unsuitable for implantation	[48]
	Methacrylate and Methacrylamide + Fibronectin	Primary RPE	None	AMD	+ Similar results as those obtained on explanted lens capsule - Altered phenotype of the cells which could be due to the age of the donors (65–70 years old)	[74]
Synthetic materials	Parylene-C + Matrigel or vitronectin	hESC-derived RPE	1) Nude rats 2) RCS rats 3) Yucatan minipigs + Clinical trial (Phase I and IIa)	AMD	+ No immune reaction nor tumour formation + Preservation of the ONL + Survival and functionality of the RPE for up to a month + Improved visual acuity with better detection of light intensity + Promising results of the clinical trials (see Table 4)	[79–86]
	PCL + integrin-binding peptides	ARPE-19	None	AMD or RP	+ Functionalization does not affect the fiber diameter but lowers the contact angle - Low characterization of the cells, notably monolayer formation - Use of the ARPE-19 cell line, unsuitable for implantation	[92]
	PBSu + Laminin 521 and collagen IV	hESC-derived RPE	None	/	+ Complete optimization of the material - No RPE monolayer observed, with poor RPE characterization	[87]
	PDMS + Ammonia gas plasma	ARPE-19	None	AMD	+ PDMS is widely used in medical devices notably in ophthalmology + Air plasma treatment increases wettability enhancing cell growth - Use of the ARPE-19 cell line, unsuitable for implantation	[76]
	Pectin-PHB	ARPE-19	None	/	+ Tunable hydrophobicity and mechanical properties according to Pectin/PHB ratio - Only 2D culture of non-confluent RPE, with low characterization of the cells	[91]

(*continued on next page*)

Table 3 (*continued*)

Material	Cell type	In-vivo and clinical translation	Targeted disease	Outcomes and limits	Ref#
				- Use of the ARPE-19 cell line, unsuitable for implantation	
PET + Laminin and collagen IV	hESC-derived RPE	1) Chinchilla-Bastard Hybrid and Dutch-Belted rabbits 2) Cynomolgus monkeys	AMD	+ Stability of the graft even upon intercontinental cell shipment (from Germany to Singapore) + RPE survival for a month along with photoreceptor preservation and *in vivo* phagocytosis	[61,62]
PET + Human placenta ECM	Adult human stem cell RPE (hRPESC)	1) Chinchilla-Bastard Hybrid rabbits 2) Cynomolgus monkeys	AMD	+ RPE survival for up to 3 months, with better survival upon local immunosuppression compared to systemic + Absence of cellular proliferation + Maintenance of the photoreceptors and capacity of phagocytosis of POS - Non homogeneous pigmentation of the cells	[59,60, 128]
PET	hfRPE	Chinchilla-Bastard and New Zealand White rabbits: acellular samples only	AMD	+ Best cellular phenotype on 200 nm fibers (pigmentation, morphology, adherence) - Lack of *in vivo* cellularized implantation to study graft efficiency - Membrane porosity does not allow proper nurturing of the photoreceptors	[90]
PHBV8	D407	None	DME, RP, AMD	+ Material degrades as D-3-hydroxybutyrate, constituent of human blood + Increase of the hydrophilicity and decrease of the roughness with the plasma treatment	[75]
PI + Laminin	hESC-derived RPE	Albino New Zealand White rabbits	AMD	+ PI clinically approved in several ophthalmic applications + Feasibility of transplantation and no obvious sign of inflammation or retinal atrophy - Loss of pigmentation with time, mononuclear cell infiltration and retinal atrophy: rejection of the transplanted cells and xenograft induced inflammation, even with immunosuppression	[70,71]
PLGA	Primary RPE	None	AMD or Stargardt disease	+ Improved morphology, monolayer formation (vs. multilayer) and microvilli development on the fibrous substrate + Similar results obtained with electrospun collagen and electrospun PLGA suggesting that the structure is more than the material itself	[88]
PLGA	hiPSC-derived RPE	1) Nude rats 2) RCS rats 3) Pigs with laser induced RPE injury	Dry AMD	+ Cell survival with maintenance of their phenotype upon implantation + Maintenance of the photoreceptors + Low inflammatory response and no tumour formation - Results similar to cell injection - Missing protocols for material characterization	[73]
PLGA or PLLA	hfRPE	None	/	+ FDA approved material - Poor characterization of cellular phenotype and behaviour	[72, 170]
PLGA; PLLA or PLDLA or PCL + Laminin	Primary RPE	In RCS rats: acellular PLLA samples only	Dry AMD	+ Best cellular behaviour on PLLA motivating its implantation + No excessive immune response observed up to 4 weeks - Lack of *in vivo* cellularized implantation to study graft efficiency	[89]
ePTFE + Ammonia plasma treatment or *n*-heptylamine coating	ARPE-19 and Primary RPE	None	AMD	+ Well-established biocompatibility and biostability + Hydrophilicity improved by plasma treatment allowing cell adhesion and monolayer formation - Only a few results with the primary RPE	[76,78]

Abbreviations: hAM: human amniotic membrane; HRP: horseradish peroxidase; PBSu: polybutylene succinate; PCL: Polycaprolactone; PDMS: polydimethylsiloxane; PEG: polyethylene glycol; PET: polyethylene terephthalate; PHB: polyhydroxybutyrate; PHBV8: Poly(hydroxybutyrate-*co*-hydroxyvalerate); PI: Polyimide; PLDLA: Poly(D,L-lactic acid); PLGA: poly(L-lactic-*co*-glycolic acid); PLLA: poly(L-lactic acid); ePTFE: expanded polytetrafluoroethylene; SF: silk fibroin; RCS: Royal College of Surgeons; NHP: non-human primates; RP: Retinitis pigmentosa; POS: photoreceptor outer segments.

its fiber diameters greatly influence both the proliferation rate and the morphology of the cells [90]. hfRPE cells express typical markers such as RPE65, ezrin, bestrophin and CRALBP and show a polarized secretion of VEGF and PEDF [57]. With long culture duration, in the range of 2–3 months, hfRPE cells are able to form tight barriers, as shown by the expression of tight junctions revealed by ZO-1 staining [90] and the evaluation of the TER resulting in particularly high values, with an increase from 200 $\Omega\bullet cm^2$ to 1000 $\Omega\bullet cm^2$ over 55 days in the study of Stanzel et al. [59] and a mean TER of 501 $\Omega\bullet cm^2$ for the model of Maminishkis et al. [57]. The hfRPE cells are cultivated on placenta ECM coated Transwell in both models. Interestingly, improvement of hfRPE ability to form a tight barrier can be mediated by the co-culture with appropriate ECs, as it was demonstrated by co-culturing hfRPE cells with fetal choroid endothelial cells at different maturation stage (P5 vs. P30) [103]. Results showed an increase in gene expression of ECM genes suggesting a regulation of the basement membrane assembly and consequent maturation of tight junctions (increased co-localisation of ZO-1 and occludin) and enhanced barrier function (TER increased values from less than 200 $\Omega\bullet cm^2$ to around 800 $\Omega\bullet cm^2$ between the monoculture and the co-culture, after 14 days). Concerning the

pigmentation of the hfRPE cells, it was reported early on that the hfRPE cells present intracellular melanosomes [72], with the pigmentation intensity varying with the culture duration. Indeed, Maminishkis et al. reported that the pigmentation decreased during the first divisions, suggesting that the daughter cells share the original pigment content, but it started to increase after a few weeks and reached the original level after 30 days [57]. A similar observation was made in another model in which the cells were fully re-pigmented after 6–8 weeks [59].

Despite their many advantages compare to cell lines, the major limitations of the hfRPE cells are the poor availability and, more importantly, the ethical concerns rising from the use of human fetal tissues.

4.1.1.2.2. Human adult RPE cells. One of the first extraction and culture of haRPE cells dates back to the 1970's with the study by Mannagh et al. whose method is still used nowadays [114]. They made several fundamental observations on the culture of haRPE cells. First, the authors noted that the viability of the cells is inversely proportional to the age of the donors, with 75% success under 60 years old versus 58% over 60 years old, highlighting the age of the donor as a key parameter in culture success. Secondly, the cells were able to form a confluent pigmented monolayer and survived for three to six months. However, they also identified several drawbacks such as loss of pigmentation with each cell division, and the spontaneous transformation of haRPE cells into cell lines, characterized by a change in morphology and an accelerated growth, which occurred in 7 cases over the 119 primary cultures.

Since the pioneer works, several studies have employed haRPE cells for oBRB modelling [78,88,89,118,123]. In several studies, a group analysed the effect of surface modification of ePTFE membranes by plasma polymerisation or by ammonia plasma treatment on the behaviour of primary adult RPE cells, without mentioning of the age of the donors [76,78,118,124]. If a first study focused on the attachment, morphology and proliferation of the cells [118], in a second study, Kearns et al. characterized in more depth the haRPE cells, with evaluation of the presence of ZO-1, *N*-Cadherin and occludin, and the analysis of the ECM production (laminin 111, collagen type I and IV and fibronectin) [78]. With experiments that lasted up to 28 days, they proved that although the support surface chemistry resulting from plasma polymerisation or ammonia plasma treatment is very different, they both support a functional monolayer of RPE and the underlying produced ECM is similar in the long term [78]. However, the characterization of the cells remained quite poor, notably lacking phagocytosis evaluation or TER measurement.

The latter was evaluated by Mennel et al. who used haRPE cells harvested from human eyes, obtained from a cornea bank and cultivating on Millicel-PCF (Millipore Corporation, USA). In this study, cellular characterization was solely based on the morphology analysed by transmission electron microscopy and on TER measurement, with values around 30 $\Omega\bullet cm^2$ which is far from the physiological value (150 $\Omega\bullet cm^2$). Thus, the monolayer formed by the haRPE cells has weaker barrier function than the natural RPE cells, as it was observed for cell lines.

Another group conducted studies to develop a RPE graft for transplantation for AMD using commercial haRPE cells, with a more complete cellular characterization [88,89]. By demonstrating the benefits of using laminin coated electrospun membrane, they showed that the haRPE cells were able to adhere and proliferate on the studied materials. TER measurements resulted in values for the haRPE cells in the range of the native one, especially for haRPE cells cultured on PLDLA or PLLA membranes. Moreover, phagocytosis assay using polystyrene beads revealed that even if the cells were always capable of phagocytosis, the number of phagocytosed beads was higher for PLLA. The membrane material also influenced the expression of typical RPE markers such as ZO-1, MERTK, PEDF, VEGF, BEST1, PMEL17 and RPE65, with enhanced expression on PLLA.

Thus, haRPE cells recapitulate the principal RPE markers and functions, but special care is required on the choice of the material to be as close as possible to the native RPE. Nonetheless, as for hfRPE cells, one major limit of haRPE is still the availability and the accessibility to donors.

4.1.1.3. Stem cell-derived RPE cells. Pluripotent stem cells include three types that we can distinguish based on their origin: adult, embryonic and induced pluripotent stem cells. In this section we focus on their application to model the oBRB. Differentiation protocols to obtain RPE cells from the different types of stem cells is out of the scope of this review and the reader can refer to the previous reviews on this specific subject by Bertolotti et al. [125], Leach & Clegg [126] and more recently by Dehghan et al. [127].

4.1.1.3.1. Adult human RPE stem cell derived RPE cells. RPE stem cell (RPESC) derived RPE are at the crosswalk of the haRPE cells (section 4.1.1.2.2) and the hiPSCs-derived RPE cells (section 4.1.1.3.3) and were first reported by Salero et al. in 2012 [128]. In healthy adult oBRB, the RPE cells are dormant and non-proliferative. However, in some diseases such as proliferative vitreoretinopathy, adult RPE cells plasticity has been observed, proving that adult RPE cells can somehow be reactivated. By extracting adult RPE cells from both young and elderly donors (up to 99 years old), Salero et al. demonstrated that a subpopulation of RPE cells can be activated *in vitro* to self-renewing cells, capable of growth. Remarkably, the age of the donor didn't impact the cell growth with a doubling rate of 2 days, up to 6 to 8 passages. During the proliferation, the cells expressed pluripotency markers (*c*-Myc and KLF4) [128]. After reaching confluence the cells regain their cobblestone morphology. These RPE cells obtained from the proliferation of RPESC expressed important markers of RPE cells (polarization, pigmentation, Ezrin, BEST, MITF, RPE65, CRALBP, MCT1, ZO-1) and when implanted on a PET membrane in rabbits, they survived up to a month [59]. Later on, the same graft was implanted in Non-Human Primates (NHP, *Macaca fascicularis,* Cynomolgus) where the cells kept RPE hallmarks (phagocytosis, RPE65, CRALBP) upon implantation with absence of both proliferation and apoptosis [60]. These cells were also used to develop two disease models following two distinct approaches. First, by using RPE cells from dry AMD patients to obtain RPESC-derived RPE cells to study the disease mechanism and the potential use of nicotinamide as treatment (see section 4.2.2) [129]. Second, in an attempt to mimic and study neovascularization, RPESC were cultivated in the presence of HUVECs to study angiogenic factors and mediators of neovascularization (see section 4.2.2) [104].

4.1.1.3.2. Human embryonic stem cell derived RPE cells. The differentiation of human embryonic stem cells (hESC) to generate various cell types started in the late 1990's [130] and one of the first reports of hESC-derived RPE cells (hESC-RPE) dates back to the early 2000's [131]. In this pioneer study, the authors characterized the RPE cells derived from 12 different hESC lines. They showed that, on gelatin coated plates, the cells could be cultured up to 9 passages and, although the cells would lose their morphology and pigmentation at first, they recover them when reaching confluency, as it is also observed for hfRPE cells for instance [57,59]. Around 90% of the hESC-RPE cells population were capable of phagocytosis and the cells expressed typical RPE markers such as CRALBP, PEDF, bestrophin and RPE65. The authors used transcriptomics to compare hESC-RPE cells with hfRPE cells and with previously published data on ARPE-19 and D407 cell lines [132]. The transcriptional identity of the hESC-RPE cells revealed to be closer to hfRPE cells than to ARPE-19 and D407 cell lines. They also identified well-substantiated RPE specific genes present in the hESC-RPE cells and in the hfRPE cells but absent from the ARPE-19 (1186 genes) and from the D407 (1452 genes) cell lines.

Since then, many studies have used hESC-RPE cells to model the oBRB, mainly for cell therapy applications [61–64,70,71,80–84,93,94,99] but also for drug development [56]. Consistent with the results in the aforementioned pioneering study, the hESC-RPE cells expressed

multiple RPE markers and are capable of phagocytosis, notably when cultivated on human amniotic membrane [94], on laminin coated synthetic polyimide [70], on vitronectin- laminin- or collagen IV-coated PET inserts [56,62,63], on RGD-alginate hydrogels [64], and on collagen coated silk fibroin [99]. The hESC-RPE cells formed a monolayer with tight junctions (ZO-1 marker), but TER values differed between studies: from 40 to 80 Ω•cm^2 [70] to values above 200 Ω•cm^2 [61] passing by values in the range of the native one (100–150 Ω•cm^2) [56]. The difference can probably be explained by different culture duration as it was reported for hfRPE cells. Indeed, if the culture duration is not detailed in the study by Subrizi et al. [70], Peng et al. [56] obtained TER physiological values after 6–8 weeks in culture whereas Ilmarinen et al. [61] obtained higher TER values with culture duration up to 20 weeks, giving more time for the RPE monolayer to mature.

Several models using hESC-RPE cells have reached pre-clinical studies and have been implanted in animal models. The hESC-RPE grafts have shown promising results in Royal College of Surgeons (RCS) rats before uncomplete retinal degeneration, with increased photoreceptor survival and consequently improvement of visual acuity [80,94]. Ilmarinen et al. conducted in-vivo studies in rabbits (Chinchilla-Bastard hybrid and Dutch-Belted) and showed the benefits of a differentiation of the hESC in xeno-free conditions to limit the immunogenicity of the graft and improve the survival of the RPE cells [61]. They then implanted the graft in immunosuppressed Cynomolgus monkeys with a mechanically disrupted oBRB and observed preservation of photoreceptors over a month with an efficient phagocytosis by the implanted RPE cells [62]. One crucial risk of using stem cell-derived RPE cells is the formation of a teratoma due to remaining contaminating stem cells in the graft. Nude rats or nude mice have been used to assess the risk of teratomas formation by either implanting the graft in the subretinal space [80] or under the skin, as the subcutaneous route represents the worst-case scenario [93]. In both cases, over respectively 12 and 6 months, no teratoma was observed in the nude animals. These pre-clinical trials lead the way to several clinicals trials that we discuss in section 4.3.3.

Once the risk of teratoma put aside, two main concerns arise from the use of hESC for RPE modelling: the availability of the cells and, most importantly, the ethical concerns rising from the use of cells derived from human embryo. Affecting only the models designed for cell therapy, a third concern regards the immune reaction due to the mismatch of the human leukocyte antigen (HLA) of the RPE graft and the patient, leading to a need for local to systemic immunosuppression [93].

4.1.1.3.3. Human induced-pluripotent stem cell derived RPE. These hESC-RPE cells limits can be overcome with the use of human induced pluripotent stem cells (hiPSC), since they can either be derived from the own patient's cells notably for disease modelling or from cells in biobanks, for cellular therapy. For the latter, numerous strategies are currently under study to obtain "fit-for-all" iPSC by developing biobanks with enough HLA haplotypes to supply HLA-matched iPSC to a wide patient population [133].

The first hiPSCs were reported by the group of Shinya Yamanaka in 2007 [134] and the first RPE cells derived from hiPSCs (hiPSC-RPE) date back to the late 2000's [135,136]. In these studies, they compared the hiPSC-RPE cells with hfRPE cells and hESC-RPE cells, already established at the time, and showed that there was no difference in the main RPE markers between those cell types.

Since these early developments, multiple oBRB models have used hiPSCs, most frequently derived from dermal fibroblasts [65,98,111–113,137–139]. The use of hiPSCs has notably enabled the development of multiple disease models by deriving hiPSCs-RPE cells from fibroblasts from patients with retinal diseases [58,65,66,98,112,140]. Since hiPSCs derived from elderly donors present an accumulation of mitochondrial DNA mutations, especially when derived from dermal cells, other types of cells have been investigated to generate hiPSCs-RPE cells, such as CD34$^+$ peripheral blood cells [73,95]. As for hESC-RPE, the hiPSC-RPE express typical RPE markers such as RPE65, BEST1, VEGF, PEDF, CRALBP, Ezrin, MERTK, PMEL and MITF [65,73,95,98,138,140] and secrete ECM proteins notably collagen IV [65,73,95,112,113,138] and VI [112]. Moreover, they can form tight junctions with a TER close to 150 Ω•cm^2 [138,140]. This value was reported to increase up to 500 Ω•cm^2 in the presence of a dense choriocapillary-bed [113], and up to 1000 Ω•cm^2 when extending cell culture from 7 to 10 weeks [73]. hiPSC-RPE also present lasting pigmentation and are capable of phagocytosis [58,73,95,98,140]. To fully characterize hiPSC-RPE gene expression, the expression patterns of 154 "hallmark" genes was studied and the authors demonstrated that hiPSC-RPE were similar to human fetal RPE [65].

As for hESC-RPE cells, the risk of tumour formation was assessed after hiPSC-RPE cells implantation in immunocompromised rats and in RCS rats without demonstrating any teratoma formation [65,73]. So far, hiPSC-RPE grafts have been implanted in various animal models such as RCS rats [65,73], pigs with laser induced injury [73] and Cynomolgus monkeys with vitreous detachment [65] with promising results in terms of inflammation, maintenance and phagocytosis of photoreceptors, preservation of the outer nuclear layer and response to visual stimuli. These encouraging results in preclinical trials lead to several clinical trials detailed in section 4.3.3.

4.1.2. Endothelial cells

In recent years, strategies to prepare more physiologically relevant constructs to model and treat the oBRB have focus on the co-culture of RPE cells with ECs. However, compared to RPE cells, the availability of choriocapillary cells is more limited, notably for the cell lines and for primary cells. Some protocols described the generation of primary choriocapillary cells derived from human donor eyes [141,142]. Unfortunately, they are characterized by limited cell viability in culture. More recently, an immortalized choroidal endothelial cell line has been established using temperature-sensitive simian virus large T antigen [143]. This cell line could be culture at 33 °C for 27 passages. Another immortalized choroidal cell line was generated by Giacalone et al. using a specific endothelial cell promoter [144]. However, the weakness of these protocols has limited the use of human eye donors as a reliable source for choroidal cell lines. A commercial human choroidal endothelial primary cell line that can be maintained in culture for up to 12 passages is currently available (Celprogen Inc.), but, to our knowledge, it has not yet been used for development of BRB model. Thus, due to the low availability of choroidal cell lines, most co-culture models to date have relied on human umbilical vein endothelial cells (HUVECs) and hiPSC-derived ECs.

4.1.2.1. Human umbilical vein endothelial cells (HUVEC). The umbilical cord presents two arteries and one large vein that can be treated with collagenase to harvest the ECs lining this vessel. The cells can then be cultured and amplified following classical 2D culture. This is a non-invasive, costly reduced and easy source of primary ECs, free of ethical concerns. Moreover, these cells are now commercially available in several cell companies. This explains why HUVECs are the first choice to prepare pre-vascularized tissue models, not only in the field of retinal engineering [145]. In monoculture, these cells do not recapitulate oBRB-specific cellular properties, such as fenestrations that ensure proper retinal functions and mediate the diseases where the choroid plays a pivotal role, as described in section 2. The differences of HUVECs with human retinal and choroidal endothelial cells were investigated by the comparison of their gene expression profiles [146]. HUVECs presented upregulated expression of genes implicated in embryonic and neuronal development, cell membrane components and ECM. In comparison, genes involved in immune responses, signal transduction and cellular responses to stimuli were upregulated in ocular microvascular endothelial cells. Unfortunately, the study did not specifically compared HUVECs gene expression versus choroidal endothelial cells. In any case, differences in genes involved in immune responses could be particularly

relevant when developing diseased models due to their implication in wet AMD and diabetic retinopathy, for instance. Yet, the studies to model the oBRB with HUVECs do not delve into immune aspects so it is difficult to know if the co-culture with RPE cells and other support cells contributes to cell maturation in this sense, as it occurs for fenestrations. Indeed, by culturing HUVECs with RPE cells numerous groups have reported changes in the HUVEC phenotype with the apparition of fenestrations, highlighting the important cell-cell communication between RPE cells and ECs [101,102,112] (see section 4.2.3). Mammalian primary endothelial cells in co-culture were chosen by Hartnett et al. [100] and Benedicto et al. [103] who worked with bovine and mouse choroidal cells respectively. Interestingly, in the latter work by comparing the exposition of RPEs to choroidal or HUVECs conditioned medium the results suggested that both cell types secreted angiocrine factors that enhanced RPE barrier function.

Based on these results, it is legitimate to question the *a priori* unsuitability of HUVECs for oBRB when cultured and matured in the presence of RPE cells. It would be interesting to further characterize the HUVECs under co-culture and compare them to choroidal cells gene expression and functions.

4.1.2.2. Human induced-pluripotent stem cell derived endothelial cells. The advantage of using iPSCs has already been mentioned before (section 4.1.1). In the case of co-culture models, the ability to obtain both iPSCs derived RPE cells and ECs from the same patient offers the possibility to create disease models for personalized medicine [112,113,139]. To our knowledge, only three groups have used hiPSCs-derived ECs, characterized by the expression of CD31, ETV2 and vWF markers [112,113,139]. Cell phenotype of differentiated cells differed from choroidal cells, with lack of fenestra. But as for HUVECs, co-culture with iPSCs-RPE cells in 3D induced choroidal fate with fenestration formation characterized by the fenestration-associated protein plasmalemma-vesicle-associated protein (PLVAP) [112,113], and increased expression of maturation markers, as well as genes related to RPE-choroidal homeostasis and BM formation [113].

4.2. BRB models developed for in vitro applications

4.2.1. Material considerations for in vitro models

Many oBRB models have been designed specifically for *in vitro* studies, and some of them focus solely on the RPE cell layer [53,54,56,58,98,117,123,129,131]. In those cases, as they were mostly designed for disease modelling or drug screening, material development and characterization were put aside to solely focus on the RPE cell behaviour. These models are thus often based on commercially available materials such as Transwell insert or even culture plates, with, in most of the cases, an additional protein coating.

Material design gained relevance with the recent development of co-culture *in vitro* models, including both RPE and choroid cells. Few models cultivated the two cell types in monolayer on each side of a membrane made either with natural material as human amniotic membrane [101] (Fig. 2.1) or with synthetic material as PDMS [106]. To recapitulate the 3D architecture of the ECs, several studies have used hydrogels to form vascular 3D structures. These hydrogels have been made of collagen type I [108], gelatin/fibrinogen using bioprinting [113], fibrin [110], collagen I/fibrin [111], methacrylated hyaluronic acid [109] and PEG with RGD-adhesive peptides [112], either in microfluidic chips [108,110,111] (Figs. 2.2 and 2.3) or in culture wells [112]. The RPE monolayer can then be formed by seeding the cells either directly on top of the hydrogel [110–112] or on a membrane placed on top of the gel made of electrospun silk fibroin [109], polyester [108] or vitronectin coated electrospun PLGA [113]. If the authors took special attention in the choice of the material for the co-culture *in vitro* models, material characterization was often absent. Only the overall dimensions of the system are consistently reported. If the human choroid is approximatively 200 μm thick and is separated from the RPE by the 4 μm thick BM, the dimensions observed in the co-culture models are usually higher, from 400 μm to 1 mm for the choroid (400 μm - Paek et al. [111]; 500 μm - Arik et al. [108]; 500 μm-1mm - Komez et al. [109]; 800 μm - Chung et al. [110]), and from 10 μm to 300 μm for the BM (10 μm - Arik et al. [108]; 25 μm - Komez et al. [109]; 300 μm - Chung et al. [110]). Two recent models successfully modelled the entire oBRB with a total thickness around 50 μm, smaller than the physiological thickness (43 μm total for Manian et al. [112], and around 50 μm with 4–10 μm membrane for the BM for Song et al. [113]). Thus, in the current *in vitro* models, no investigation of the mechanical properties, wettability, porosity, permeability or topography are usually conducted, even if those parameters are crucial for the cellular behaviour. Future studies should thus pay particular attention to the characterization of their systems to ensure the relevance of their models.

4.2.2. Pathological models

In vitro disease models allow the understanding of new pathology mechanisms and the pre-screening of potential therapeutics, thus reducing the need for animal experimentation. In the latter years, disease modelling increased thanks to the use of patient-derived hiPSCs allowing the study of deleterious cellular behaviour. Several retinal diseases have thus been modelled over the years, the most studied being AMD, both in its wet and dry forms.

4.2.2.1. AMD models. Different AMD models have focused either on the RPE alone or on the interactions between the choroid and the RPE during the course of the disease.

To better understand the AMD onset, Moreira et al. studied the effect of BM aging on the POS phagocytosis by the RPE cells [46]. BMs were extracted from young (<46 years old - control) or old donors (>74 years old) and were used as a support to cultivate ARPE-19 cells. The results highlighted that the cell phagocytosis ability decreased with age, concluding that the natural aging of BM components could play a role in the onset of AMD. Another AMD RPE model studied the inflammation mechanisms in dry AMD and the therapeutic effect of nicotinamide [129]. To do so, RPE cells were derived from hiPSCs obtained from human RPE cells and corneal fibroblasts of AMD patients between 73 and 93 years old (with control from healthy 71–91 years old donors). If all cells (control and diseased) expressed classical RPE markers, only cells from patients produced higher levels of drusen-related proteins and of complement and inflammatory factors. Addition of nicotinamide improved the disease-related phenotypes, thus targeting nicotinamide-regulated pathways could be a potential strategy for AMD treatment. Pathological RPE derived from AMD hiPSC (and healthy age-matched control) were cultured on nitrite-modified ECM, to mimic AMD-altered ECM [140]. If AMD RPE cells had similar morphology, markers expression, TER and phagocytosis capability as the control cells, they demonstrated a downregulation of several genes responsible for metabolic-related pathways and cell attachment and a reduction of mitochondrial functions, giving new insights on the AMD mechanisms.

By including the choroidal compartment, several co-culture devices were able to model even more closely the pathological mechanisms. Chung et al. studied choroidal neo-vascularization in wet AMD by generating, in a microfluidic chip, a vascular network in a fibrin hydrogel, on top of which were seeded the RPE cells [110] (Fig. 3.1A). The vascular network and the RPE monolayer were separated by a 300 μm blank fibrin hydrogel to observe the formation of angiogenic sprouts disrupting the RPE monolayer. This platform was also used to analyze the regression of the pathological angiogenesis by application of bevacizumab (Avastin^{R}), the clinical drug used in wet-AMD, showing the potential of the chip for drug screening (Fig. 3.1B-E).

AMD and related macular dystrophies (MD) were further modelled by including mesenchymal stem cells (MSC) in addition to EC and RPE cells, all derived from AMD patients' iPSCs [112]. The ECs were

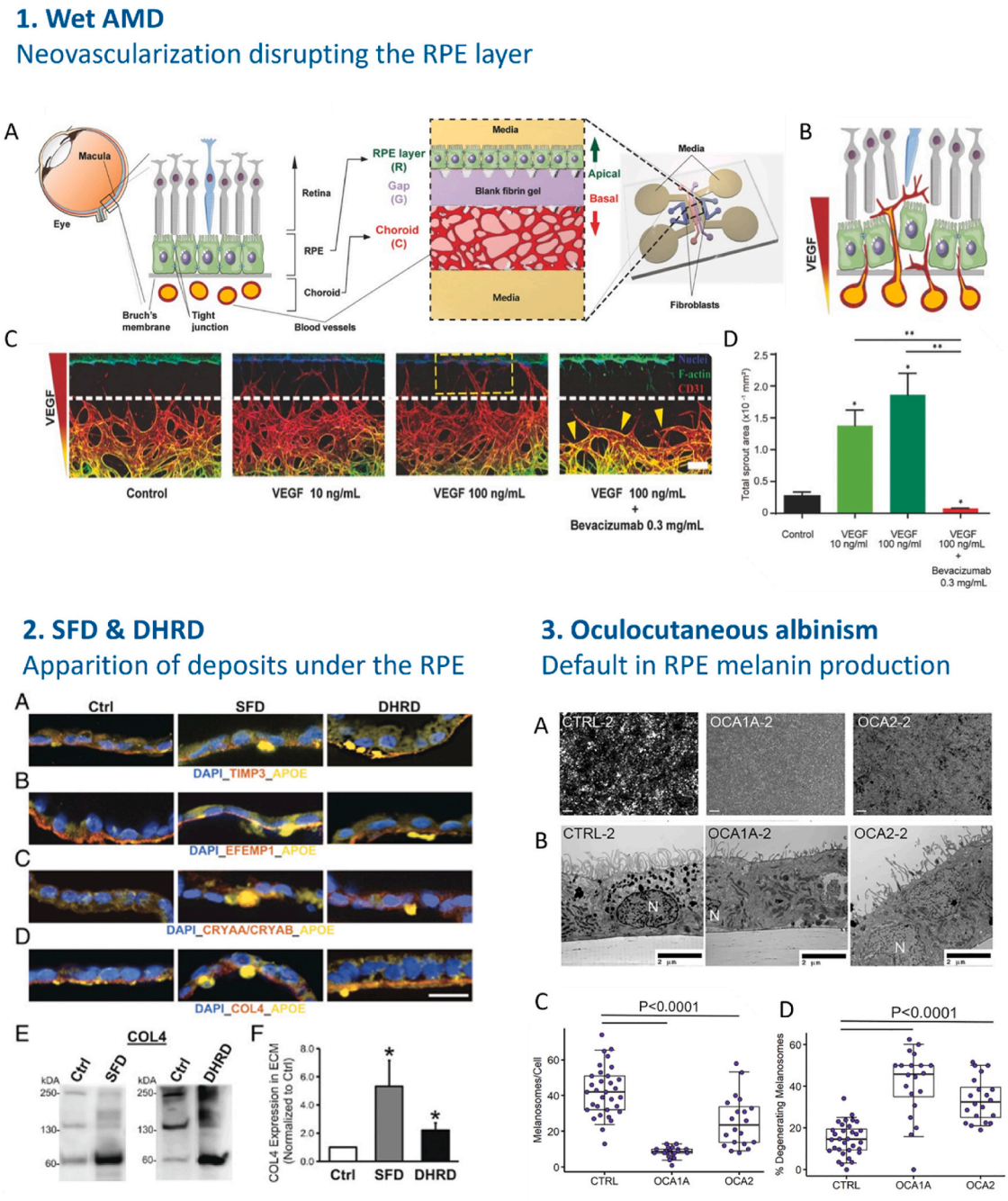

Fig. 3. oBRB disease modelling. 1/ Co-culture model of the choroidal neovascularization (CNV) in wet-AMD. (A) Scheme of the RPE–choroid complex underlying the neural retina of the eye and design of the microfluidic device to mimic it, using HUVECs, ARPE-19 and fibroblasts. (B) Schematic illustration of CNV, with the RPE layer and Bruch's membrane being destroyed by angiogenic sprouting of the choroid induced by an abnormal VEGF (vascular endothelial growth factor) gradient. (C) Representative images of VEGF treatment with or without bevacizumab. Excessive angiogenic sprouts in the gap channels were regarded as neo vessel formation. Cotreatment of VEGF with bevacizumab inhibited angiogenic sprouting. Scale bar: 200 μm. (D) Measurements of the area of angiogenic sprouting in the gap channel. The boundary of the gap and choroidal channel is indicated as a dotted line in (C). *P < 0.05. n = 3 for each condition. Adapted from Chung et al. [110] with permission of John Wiley and Sons. **2/ Mono-culture model of SFD and DHRD.** Formation of sub-RPE deposits with drusen-like composition underneath aged (D90) SFD and DHRD hiPSC-RPE cultures. (A–D) Confocal images of cellular cross-sections displayed the presence of TIMP3-APOE–positive (A), EFEMP1-APOE–-positive (B), CRYAA/CRYAB-APOE–positive (C), and APOE-positive deposits underlying basement membrane marked by COL4 (D) in SFD and DHRD hiPSC-RPE cultures. Scale bar: 25 μm. (E–F) Quantitative Western blot analyses revealed increased amount of COL4 protein in the ECM underlying SFD and DHRD hiPSC-RPE cultures compared with Ctrl hiPSC-RPE cultures at D90. Data are presented as mean + SEM. *P ≤ 0.05. Adapted with permission from Galloway et al. [147]. **3/ Mono-culture model of oculocutaneous albinism.** hiPSC-RPE from OCA1A and OCA2 patients, cultured on Transwell recapitulates the disease characteristic pigmentation defects, by demonstrating various amounts of melanin and melanosomes (A–B) Brightfield microscopy images and transmission electron microscopy of CTRL-, OCA1A-, and OCA2-hPSC-RPE monolayers. Scale bar: 200 μm and 2 μm respectively. (*C*–D) Quantification of the number of melanosomes per cell and quantification of degenerating melanosomes in CTRL-iRPE (N = 32), OCA1A-iRPE (N = 20), and OCA2-iRPE (N = 20), where N is the number of unique TEM images represents pooled data from a single differentiation event of four different lines in each group. The horizontal lines in the box plots indicate the median, the boxes indicate the first and third quartiles, and the whiskers indicate the 5th and 95th percentiles. Student's *t*-test was used to determine p values. Adapted from Georges et al. [58] with permission of Elsevier.

encapsulated in a PEG-RGD hydrogel to form the choriocapillaris network while the RPE cells formed a monolayer on the gel surface. This platform showed the important contribution of both the RPE cells and MSC to the formation of fenestrated microvasculature-like structure in the oBRB formation and their role in the progression of AMD/MD pathologies. Interestingly, they demonstrated that choroidal neovascularization and capillaries atrophy can be initiated solely by alterations in RPE-secreted factors.

Song et al. investigated a different approach by supplementing their ECs-RPE co-culture model with pericytes and fibroblasts to promote vascularization [113]. They used their 3D platform to model both dry and wet AMD. The first was induced by a treatment with complement-complement human serum which induced *in vitro* drusen formation by lipid deposit formation followed by RPE atrophy, capillary degeneration, and loss in the barrier resistance, thus recapitulating dry AMD phenotype *in vitro*. Wet AMD was generated using two different approaches. The first consisted in modelling the effect of hypoxia by a treatment of ML228, which activates the HIF-1α RPE transcription factor leading to increased VEGF secretion. The second approach relied on RPE cells derived from an iPSC line genetically modified to overexpress STAT3, a pro-angiogenic and pro-inflammatory factor in RPE. Both approaches lead to a complete disruption in the RPE monolayer, notably characterized by a drop in the TER and by a hyperproliferation of the choroid capillaries expanding towards the RPE monolayer. Once they validated their platform, they showed that their model could also be used as a drug testing device, by assessing the recovery of the wet-AMD form after Bevacizumab treatment.

Thus, different approaches successfully mimic different symptoms and mechanisms of AMD, offering different platforms for drug testing applications. One limitation, notably for the last two more complex models, is the lack of circulating flow in the formed vasculature which could impact the distribution and action mechanisms of tested drugs. Current microfluidic advances are encouraging for the future incorporation of flux in complex 3D models.

4.2.2.2. Other disease models. Diabetic macular edema was often modelled by inducing hyperglycemia and hypoxia on RPE cell culture [49–53]. The studies by Maugeri et al. revealed that vasoactive intestinal peptide (VIP), pituitary adenylate cyclase-activating polypeptide (PACAP) and caffeine counter the effects of the disease whereas nicotine worthens the effect of hypoxia and hyperglycemia [49–52]. Similarly, Doganlar et al. showed that by improving TER, reducing permeability and protecting the cells against mitochondrial dysfunctions, melatonin may have a beneficial therapeutic value to revert the effect of hypoxia and hyperglycemia on the RPE cells. A co-culture model also investigated the effect of diabetes on the oBRB by cultivating, in a microfluidic chip, HUVECs and ARPE-19 cells in monolayers on the opposite sides of a porous membrane [106]. By placing the cells under low glucose concentration and hypoxia, an increased secretion of VEGF by the RPE cells caused migration of HUVECs and a subsequent breakdown of the RPE monolayer, reproducing the disease mechanism. The pathological effect of hypoxia was also investigated by Kumar et al. by cultivating RPESC in the presence of HUVECs to study angiogenic factors and mediators of neovascularization [104]. Under hypoxia, increased levels of VEGF protein and VEGF/VEGFR gene expression by human retinal progenitor cells were detected. Interestingly, co-culture with ECs had a synergistic effect under hypoxia and resulted in a significant increase of gene and protein secretion and an enhanced neovascular response.

Three less-documented retinal genetic dystrophies, Sorsby's fundus dystrophy (SFD), Doyne honeycomb retinal dystrophy/Malattia Leventinese (DHRD), and autosomal dominant radial drusen (ADRD) were studied by deriving RPE cells from several hiPSCs carrying or not mutations (2*SFD; 2*ARDR; 2*DHRD and 5 control lines) [147]. If all cells expressed typical RPE markers, the diseased cells started to form numerous sub-basal deposits after a few months in culture, with an onset depending on the disease (earlier for DHRD) and with different drusen-like composition among the different diseases (Fig. 3.2).

Recently, a model of oculocutaneous albinism (OCA), a genetic condition affecting pigmentation in the skin, the hair and the eye, has been developed [58]. iPSCs were generated from fibroblasts from patients with either the OCA1A mutation (in TYR gene, n = 2) or the OCA2 mutation (in P gene/OCA2 gene, n = 2) or from healthy controls (n = 2), and further derived into RPE cells. By comparing the pigmentation and the melanosomes activity, they showed that, compared to the control, OCA2 RPE cells demonstrated a small pigmentation with only 32% of mature melanosomes (vs. 94% in control). The alterations were more severe with the OCA1 mutation, where neither pigmentation nor mature melanosomes were observed in the differentiated RPE (Fig. 3.3). Thus, this model is in line with the clinical observations and could be used to further understand the disease mechanisms and to test therapeutic strategies.

To study gyrate atrophy, Meyer et al. has developed RPE derived from gyrate atrophy hiPSC cells, from 3 patients with the A226V OAT mutation [137]. The diseased cells expressed the typical RPE markers, with levels similar to control cells. The presence of the mutation was confirmed by measuring a lower OAT activity in the patients' cells compared to the controls. However, the authors showed that the treatment of cells with elevated levels of vitamin B6, up to 600 μM, could restore OAT activity in the diseased iPSC-RPE cells, highlighting the vitamin as a potential treatment against gyrate atrophy.

Recently, Duong et al. showed the use of patient-hiPSC in the pathogenesis of choroideremia for the discovery of new treatments, notably gene augmentation therapy [21]. Cultivated on fibronectin coated Transwell membranes, the patients' hiPSC-RPE cells expressed typical RPE markers, were polarized and formed a tight monolayer with a TER higher than 250 $\Omega \bullet cm^2$. Due to the mutation in the CHM gene, the choroideremia RPE cells did not express the REP1 protein. With this model, the authors demonstrated that the lack of REP1 leads to a reduced phagocytosis by the RPE cells, an inhibition of the prenylation of Rab proteins, involved in vesicular trafficking, as well as a perinuclear accumulation of the Rab27a protein.

Thus, recent advances in the development of hiPSC-derived RPE cells have allow the modelling of various genetic diseases, to better understand their mechanisms and find potential treatments. However, so far, except for AMD, the disease models have not included any support cells, notably choroidal cells, despite the recently reported benefits of co-culture presented in the following section.

4.2.3. Lessons from the co-culture

Modelling the RPE monolayer in the presence of ECs is a relatively recent approach and the number of studies remains low (see Table 1). Nevertheless, some conclusions can already be pointed out to help the development of improved models and therapeutic implants.

One of the first studies where the impact of the co-culture in an oBRB model was assessed was done almost two decades ago [100]. Their goal was to study the effect of bovine ECs in monolayer on the barrier capability of a monolayer of bovine RPE cells, using a Transwell system and different types of cell interaction, including contact and contactless co-cultures. In this study, the co-culture with ECs led to a reduction of the barrier functionality, notably mediated by VEGF secretion. Later on and in line with this first study, negative effects of the co-culture have also been demonstrated by others. By using a model on a chip with two channels, one for ARPE-19 cells and the other for HUVECs, Chen et al. showed how HUVECs invaded and broke down the monolayer of ARPE-19 cells, invalidating the system to evaluate the effect of glucose concentration or chemical hypoxia [106]. Interestingly, Chung et al. also observed an invasive and disruptive effect, but in their case, it was caused by ARPE-19 cells, leading to choroidal vessel regression [110]. In order to counter this phenomenon and to create a model of pathological angiogenesis, authors increased the distance between the monolayer of ARPE-19 cells and the network of HUVECs by adding a blank fibrin gel

layer between them. A similar effect was reported by the team of Hasirci with a reduced EC coverage of a tree-like structure made of collagen-methacrylate when RPE cells were cultured on a porous electrospun silk membrane on top [109]. It must be pointed out that, in this last example, only contactless co-culture methods were used, with the ECs network at the bottom of the well plate and the RPE membrane held in a cell crown holder. These negative effects can be caused by the use of suboptimal materials as tissue support. As reported by Chung et al., the characteristics of the culturing device play a key role in those interactions making it possible to even reverse the pernicious effect of co-cultivation through the optimization of some biomaterial parameters [110]. Calejo et al. also demonstrated that the material porosity has an important influence on the interactions between the RPE cells and the ECs, using monolayers on opposite side of a PLA membrane [148]. They also showed the importance of the cell source. Indeed, if negative effects were observed in the co-culture of hiPSC-derived RPE cells and primary ECs, such as HUVECs, they were reduced when co-cultivating hiPSC-RPE cells with hiPSC-ECs. It should however be noted that this study focuses mainly on cell number and lacks additional cell function characterization (only CRALBP for RPE and vWF factor for ECs).

Consequently, by designing the adequate material support, along with the proper cell types, most authors have been able to develop non pathological models where the benefits of cell communication between RPE cells with ECs and/or other cell types is demonstrated.

4.2.3.1. Benefits of co-culturing retinal pigment epithelial and endothelial cells. Several works have shown how the co-culture of RPE cells in the presence of ECs improved RPE monolayer formation and maturation, with increased number of tight junctions [102], as well as cellular polarization with microvilli on the apical surface [101], resulting in improved barrier [101,103,110,111] and phagocytic activity [101,102], and increased pigmentation of the retinal epithelial cells [111]. The improvement of RPE functions is intimately related to the characteristics of the underlying ECM. In this sense, co-culture with ECs has been associated with the increase of matrix-related genes and protein deposition by RPE cells, including laminin, collagen IV, collagen VI, fibronectin and fibrillin on the basal side of RPE [102,103,111,112]. This could be mediated by the secretion of angiocrine signals by ECs as suggested by Benedicto et al. [103] who reported a new mechanism to regulate oBRB maturation by the secretion of angiocrine molecules implicated in the remodelling of basement membrane and resulting in improved barrier functions. This was demonstrated by culturing hfRPE cells in Transwell inserts with mouse fetal choroid ECs at different maturation stage (post-natal day 5 (p5) vs. p30) [103]. This study raises interesting hints for retinal tissue engineering as it shows the importance of both the ECs maturation state, particularly relevant for studies involving stem cells, and the composition of the ECM, having a major role on barrier function. Indeed, a complex model was recently developed in which 3D culture of human retinal microvascular endothelial cells (HRMVEC) and choroidal fibroblasts was performed in a fibrin and collagen gel with two perfusable endothelialized channels and combined with a monolayer of iPSC-derived RPE cells on top [111] (Fig. 2.3). The presence of the choroid caused an increase of ECM deposition, pigmentation and RPE65 expression. To note, this is one of the few studies carried out and in the presence of choroidal fibroblasts to support the choroid and under flow conditions, a factor that can also affect maturation and consolidation of the choroid.

The last work by Song et al. using also iPSCs-derived RPE cells showed the constitution of a mature epithelium when cultured on PLGA fibers in the presence of a dense capillary bed obtained by bioprinting of hiPSCs-EC with human placental microvascular pericytes and adult choroidal fibroblasts [113]. A key outcome in this work was the formation of a 2–4 μm BM-like structure between the RPE and the vascular compartment concomitant to the degradation of the PLGA support. The constitution of this natural ECM was probably enhanced by the presence of pericytes and fibroblasts in the vascular compartment and by the long-term culture of the construct (6 weeks). To our knowledge, this is the model with the highest level of cell complexity developed to date. The authors demonstrated that iPSCs-RPE expression profile greatly differs when cells are seeded on this natural ECM compared to 2D plastic substrates, highlighting the increased expression of genes implicated in the visual cycle, angiogenic and non-angiogenic genes, components of the BM and exosome assembly genes. Reciprocally to the beneficial effect of the vascular compartment on the RPE monolayer, the polarized epithelium induced fenestrations in the capillary network that attained an arterial and choroidal phenotype [113]. This result confirms the observation by Manian et al. [112] also using a 3D model with iPSCs derived into RPE cells and ECs in the presence of support cells. It should be noted that this beneficial effect of RPE cells on ECs is not exclusive of iPSCs and was reported by others before. In particular, HUVEC proliferation and survival increased when co-cultured with quiescent and confluent ARPE-19 cells [102]. Interestingly, HUVECs presented pores and caveolae-like structures [102] and, in some cases, fenestra as soon as after 72 h in co-culture [101,112]. Besides, enhanced RPE expression of antiangiogenic genes accompanied by increased secretion of anti-angiogenic factors, such as PEDF and THBS1 resulted in a reduced EC angiogenic capacity, confirmed by *in vitro* tube-formation assay, indicating a vessel stabilization role mediated by the epithelium [102].

4.2.3.2. Benefits of incorporating support cells. As already mentioned, recent studies point to the importance of including support cells in co-cultures. To date, one-third of reported co-cultured oBRB models included at least one support cell type, namely fibroblasts, including human lung [106,108,110] and primary human choroidal [111,113,139]; mesenchymal stem cells [112] and pericytes [113,139]. Studies have revealed the important contribution of fibroblasts to support the choroid networks [108,110,111,113] as well as to improve the epithelial monolayer formation [110]. These outcomes are probably mediated by the production of soluble factors and matrix proteins involved in lumen formation and stabilization of microvessels. In the recent work by Song et al., the authors went a step further by including not only fibroblasts but also pericytes in the vascular compartment [113]. In line with other studies, in the absence of support cells, angiogenesis was incomplete while it was observed by addition of fibroblasts. Regarding pericytes, the authors demonstrated their ability to promote EC migration, accelerating the formation of new vessels, and confirming their role in stabilizing the vascular network. This is without any doubt a very interesting clue for future works in the field. As for mesenchymal cells, to the best of our knowledge, they have only been used in one study whose results point to a stabilizing role in the vasculature similar to that of pericytes [112]. Notably, the incorporation of mesenchymal cells made it possible to prolong the culture of the model from 2 weeks to 2 months.

4.2.3.3. Co-culture models are suitable to mimic pathologies. Models based on co-culture have undoubtedly provided important insights into the functioning of the retina and in particular the interaction between the epithelium and the choroid. Bearing in mind that the origin of many retinal diseases resides into alterations at this level, it is not surprising that one of the main objectives of co-culture models has been, from the beginning, the fine-tuning of pathological modelling. Co-culture-based models have undoubtedly provided important insights into the functioning of the retina and in particular the interaction between the epithelium and the choroid. Thus, 2D Transwell systems [104], devices on chips [108,110,149] and more complex 3D constructions [112,113] have all proven their interest for the study of pathologies and drug evaluation as already discussed in section 4.2.2.

4.3. oBRB models developed for in vivo implantation

We are now presenting the studies aiming to develop an implant for

oBRB cellular therapy. To the best of our knowledge, all oBRB implants developed to this day do not yet integrate the choroid. Thus, this part will cover the previous strategies for RPE cellular therapy, by focusing especially on the ones having developed their own membrane instead of using commercially available products such as Transwell inserts.

4.3.1. RPE implant material and characterization

When developing a material for tissue engineering, multiple parameters need to be considered such as the nature of the material, its topography, its wettability, its porosity, its mechanical properties, its biocompatibility, and its potential functionalization to favor cellular function (see details in Table 2).

- Natural versus synthetic material

The very first step of the implant design usually focuses on selecting the appropriate material. As mentioned in section 3, multiple materials have been investigated for oBRB cell therapy. Notably, many natural

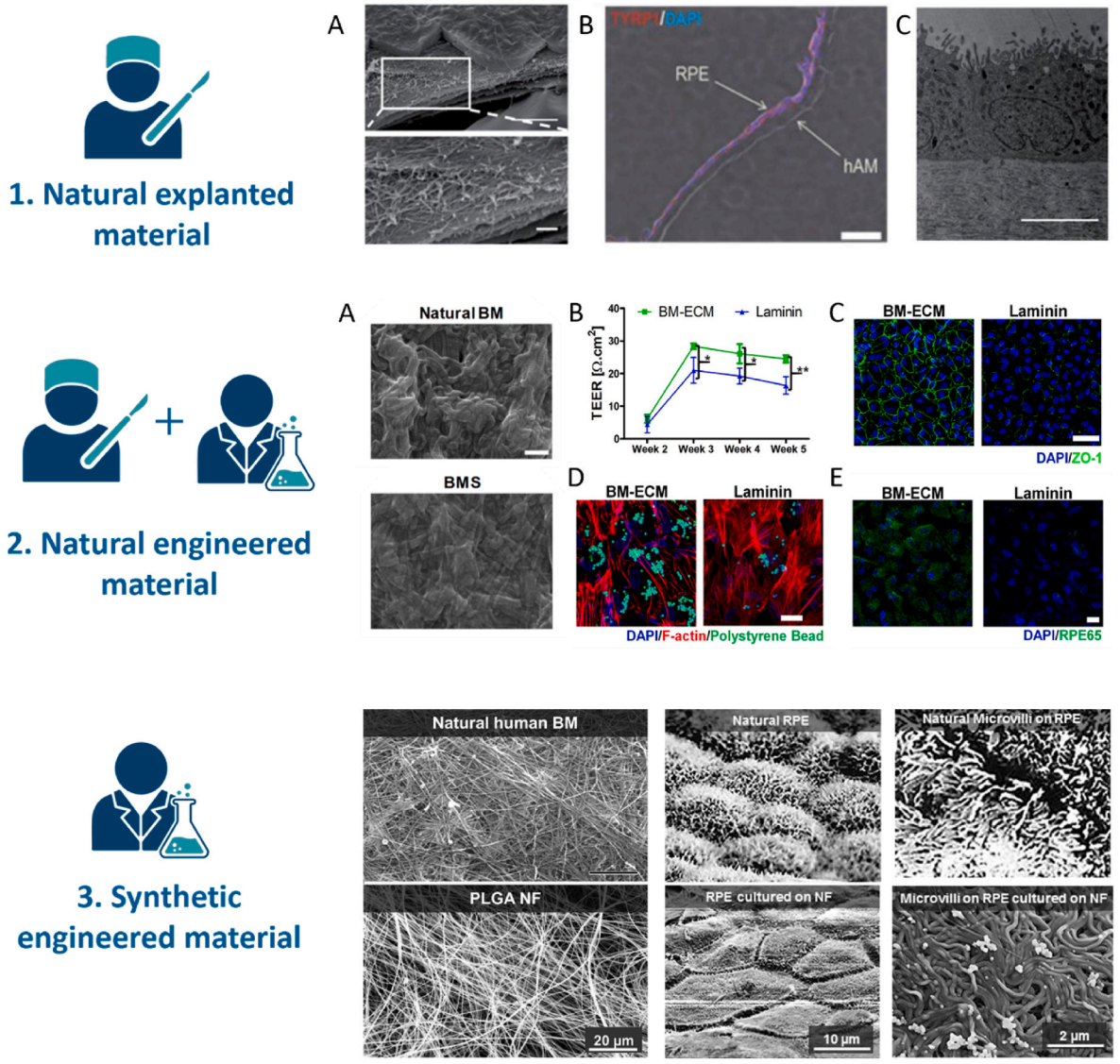

Fig. 4. Development of RPE implant for oBRB regenerative medicine. 1/ Use of a natural explanted tissue as RPE support. hESC-RPE cultured on decellularized human amniotic membrane (hAM). (A) Scanning electron microscopy images of the hESC-RPE cell sheet on the hAM scaffold: the bottom image (a magnification of the area indicated by the rectangle in the top image) shows the basement membrane and extracellular matrix fibers of the hAM scaffold. Scale bars: 5 µm (top) and 1 µm (bottom). (B) Section of the cell sheet illustrating the monolayer organization of hESC-RPE cells. Scale bar: 50 µm. (D) Transmission electron microscopy image of the hESC-RPE cell sheet. Scale bar: 5 µm. Adapted from Ben M'Barek et al. [94] with permission of The American Association for the Advancement of Science. **2/ Use of naturally sourced material, re-engineered to obtain a novel material.** Development of a 3D printed bioink from explanted porcine Bruch's membrane and PCL (BMS). (A) Scanning electron microscopy (SEM) images of BMS and natural BM. Scale bar: 500 nm. (B–E) Effect of Bruch's membrane-derived extracellular matrix bioink (BM-ECM), compared to a laminin coated Transwell, on the behaviour of ARPE-19 cells: (B) Transepithelial electrical resistance (TEER) values at various times; (C) Expression of ZO-1 for tight junction; (D) Phagocytosis capacity with polystyrene beads; (E) Expression of RPE65 for phototransduction. Scale bars: (C) 50 µm and (D–E) 20 µm. The error bars represent the standard deviation. The data were compared using Student's t-test and differences were considered significant for * $p < 0.05$ and ** for $p < 0.01$ ($n = 3$). Adapted with permission (Creative Commons Attribution 4.0) from Kim et al. [48] **3/ Development of a synthetic membrane for RPE culture**. Synthesis of an electrospun PLGA membrane (bottom line) to mimic the fibrous structure of the native BM (top line). SEM imaging of the membrane fibers structure (first column) and the structure of cultivated human primary RPE monolayer compared to the native RPE in its natural environment: as for native RPE, the haRPE on the PLGA membrane display the typical hexa/polygonal shape (second column) and are covered with microvilli on the apical side (third column). Adapted from Warnke et al. [88] with permission of Elsevier. Figure created with *BioRender.com*.

materials have been tailored to create a membrane for tissue engineering. For instance, Kim et al. created a bioink from porcine BM that successfully supported RPE culture and that has been implanted in rats (Fig. 4.2) [150]. Other natural materials, non-specific to the retina, have been investigated such as silk fibroin from *Bombyx mori* cocoons as an electrospun membrane [97,98], amniotic membrane (Fig. 4.1) [94,95] and collagen type I [69,88]. To reinforce the properties of natural materials, some studies combined them with synthetic materials as for instance hAM powder mixed with PCL [96] or PEG and horseradish peroxidase added to silk fibroin to improve porosity and permeability [99]. However, many of the reported natural materials are associated to several limitations, such as the limited availability and reproducibility, and raise ethical concerns in the need of animals or human donors.

To overcome these disadvantages, synthetic materials have been proposed such as PDMS [77], PHBV8 [75], PET [90], PLLA [72,89], PLGA [72,88,89,151], PCL [89,90,92], polyimide [70,71], Parylene-C [79] and PHB [91] (Fig. 4.2). Nonetheless, these materials present a few drawbacks too. First, there synthesis usually requires the use of organic solvents such as hexafluoropropanol or chloroform. Extra care should therefore be paid to the trace of solvent in the material before cellularization and implantation. Secondly, these materials rarely allow efficient cellular adhesion without additional functionalization. Typically, coating of the material is performed with natural proteins. Laminin (from mouse [70,89] or from human placenta [70,71]); collagen type I (from human placenta [70] or from porcine [98,99]); collagen type IV (from human placenta [70]); or complete ECM from human placenta [97] have been reported as efficient biosurfaces to enhance RPE cells adhesion on various materials. As for natural materials, such proteins are often produced using animal models, which limits their availability and raises ethical concerns. Thus, alternative functionalization strategies have been investigated such as plasma treatment [75,76,78,118], the production of recombinant proteins or the synthesis of peptides promoting cellular adhesion as laminin peptides [70]; RGD peptides [64] or integrin-binding peptides [92].

- Thickness

The thickness of an implant should mimic as closely as possible the thickness of the native tissue to avoid additional tissue disruption or damage upon implantation. Since the implants do not include the choroid, studies focused on recapitulating the RPE on the material support acting as the BM, whose thickness has been reported to be around 2–4 μm thick in the human retina [10]. Based on this, to the previously mentioned limitations of reported natural materials used as RPE support, we should add the thickness that is often too high to mimic the BM. For instance, the human amniotic membrane, used in several models [93–95], has been reported to be around 100 μm thick [95] which is 25 times thicker than the BM. However, studies have shown that the hAM implantation do not alter the overlying retina layers in non-human primates [93].

Current biofabrication material process, such as the commonly used solvent casting and electrospinning, allow for a fine tuning of the material thickness. oBRB membranes with thicknesses lower than 10 μm have thus been successfully obtained, with either natural [69,97–99] or synthetic materials [73,75,79,89,90,92] (see Table 2).

- Topography

Most of the early materials developed for oBRB cell therapy had particularly smooth surfaces. This is notably the case for hydrogels [65,74] or for materials obtained using solvent casting method [72,75,76,97]. However, due to its highly collagenous composition, the BM is characterized by fibrous surfaces [152] with fibers around 60 nm in diameter [88]. In line with this, the study by Warnke et al. showed that nanofibrous membranes were beneficial on the RPE behaviour compared to smooth films (Fig. 4.3) [88]. Indeed, by comparing electrospun PLGA membranes with casted PLGA films, they demonstrated that primary RPE cells had a better cobblestone morphology, formed monolayers (vs multilayers) and had a better polarization on the nanofibers. Liu et al. then highlighted the impact of the nanofibrous diameter on the cell behaviour by comparing electrospun membranes with fibers with diameters of 200 nm, 500 m or 1000 nm [90]. Their findings suggest that the membranes with the 200 nm fibers, the closest to the natural BM fibers diameter, are best suited for RPE cell culture, in terms of pigmentation, morphology, adherence and proliferation. Since then, many groups have developed fibrous membranes for oBRB modelling using different techniques such as heat-fusion [73], 3D printing (Fig. 4.2) [48] or most commonly electrospinning (Fig. 4.3) [88–92,96]. When reported, the average fiber diameter in these studies is usually around 300 nm [73,78,88,91,92,96] which is 5 times higher than the natural BM fibers. The study by Surrao et al. stands out with an average fiber diameter lower than 70 nm for all tested materials [89].

- Wettability

The importance of the material wettability on cellular adhesion has been extensively studied and previously reviewed and it has been reported that cell adhesion is favored on moderately hydrophilic substrates [153,154] such as collagen type I membranes whose water contact angle was reported around 80° [69]. However, most of the synthetic materials in oBRB models have higher contact angles, usually above 100° (PCL: between 92° [92] and 119° [96]; PLGA:105°; PLLA: 108° [89]; PTFE: 133° [78]) which limits cellular adhesion. As previously mentioned, functionalization is often performed on synthetic material, lowering their water contact angle. For instance, plasma treatment has been used to reduce PTFE contact angle from 133° to 68,5° [78]. This approach was also chosen to increase hydrophilicity of PLGA fibres to enhance bioink attachment and cell adhesion in the model developed by Song et al. [113]. Another strategy is to add ECM proteins to the membrane composition as demonstrated by Majidnia et al. who showed a decrease of the contact angle from 119° to 92° by addition of human amniotic membrane in PCL. Similar results were obtained by coating the membrane with adhesive peptides such as integrin-binding peptides (contact angle going from 92° to 20° on PCL [92]).

- Mechanical properties

It has become increasingly evident that the mechanical properties of a biomaterial have an important impact on cellular behaviour and tissue functionality [155]. However, discussing the mechanical properties of the oBRB membranes is challenging since their evaluation differs greatly in methodologies between the different studies. Indeed, various classical techniques have been used, mainly tensile deformation [88,91,96,99] and atomic force microscopy [71,75,78,89], and also deflection tests [79] and shear rheometry [48]. However, these methods evaluate the mechanical properties through different variables (Young's modulus, ultimate strain, ultimate tensile strength and mean roughness to name a few) and at different scales (from nanoscale to macroscale). Moreover, when the same method is used, the test parameters can differ and affect the results (characteristics of the probe in AFM for instance). Keeping in mind these major constraints to compare results, Young's modulus is usually in the range of tens to hundreds of MPa for synthetic materials such as PLGA, PLLA, PCL or PHB [88,89,91,96]. Are these values close to the physiological tissue? The rare studies analysing the mechanics of the human oBRB, and recently reviewed by Ferrara et al. [8], also used different tissue extraction and isolation methods and different mechanical testing methods. Moreover, they usually characterized either the entire retina or the entire choroid, with values characteristic of a soft tissue, lower than a 1 MPa. However, if we look at individual collagen fibers, important component of the BM, higher values, in the range of the GPa, in tensile deformation or nanoindentation, are usually reported

[155]. Thus, it is not clear to define a real target for the mechanical properties for RPE replacement. As far as we know, no study has directly compared extracted oBRB tissue with their own material by using the same methodology on the two supports, which would be in our opinion the ideal situation.

Another important aspect concerning the mechanical properties is to make sure that the implant can sustain surgical implantation. In this regard, when comparing different material compositions, the authors would generally lean towards the formulation enhancing the robustness of the implant [71,79,88,89,96].

- Permeability

Once implanted, the material will act as a barrier between the patient's choroid and the grafted cells. The membrane thus needs to be permeable enough to allow for all natural exchanges, in nutrients, growth factors and oxygen, between the fenestrated blood vessels and the RPE. One of the largest molecules involved in the RPE visual cycle, and supplied by the choroid, is the vitamin A or retinol, which, with its carrier, reaches a molecular weight (MW) around 75 kDa [156,157]. Hence, an oBRB membrane should allow the diffusion of all molecules with MW as high as 75 kDa. Permeability studies can be conducted easily by measuring the diffusion of fluorescent molecules, of various MW, across the membrane, allowing the computation of the diffusion coefficients for each MW. When more than 3 molecules are used, a linear regression of the diffusion coefficient according to the MW gives the membrane exclusion limit [157].

Yet, the permeability is still understudied and several studies used only one type of molecule, usually with a small MW. For instance, Ilmarinen et al. and Suzuki et al. conducted diffusion tests using molecules of 700 Da and 500 Da respectively, too small to be physiologically relevant [71,99].

Only a few studies conducted a complete permeability analysis, with more than 3 investigated molecules, including one with a MW above 75 kDa. For instance, by using 6 different dextran molecules of MW ranging from 4 to 250 kDa, Lu et al. proved that their parylene-C membrane has diffusion coefficients between 10^{-10} and 10^{-13} $cm^2\,s^{-1}$ and an exclusion limit of 1008 kDa, thus being adapted for oBRB application on the permeability level [79].

If the exclusion limit is an important variable to characterize the membrane, it should be kept in mind that the diffusion coefficients should be compared to the ones from the native BM, which are extremely difficult to characterize.

- Degradation

The degradation of the scaffold is particularly important in tissue engineering applications. In the case of the oBRB replacement, most of the scaffolds are made to degrade and to be replaced by RPE-produced ECM with time. In this perspective, most of the previously mentioned studies selected biodegradable materials (PLLA, PLGA, PCL, PHB-V8), except Parylene-C, PDMS, polyimide and ePTFE. Material degradation rate will highly depend on its thickness and its mechanical properties. Once implanted, it will also depend on the patient's immune reaction to the graft. In general, the degradation of oBRB implants is still poorly studied and several non-comparable techniques have been used notably enzymatic degradation [99] or simple incubation at 37 °C in PBS [96].

The design of oBRB implants for cellular therapy have greatly evolved since the early models developed nearly two decades ago. The development of new materials and new functionalization strategies have improved the material properties while reducing the need for animal or human donors. Moreover, technical advances have enabled the synthesis of more complex membrane in terms of structure and topography within thinner thicknesses. However, rare are the studies conducting a thorough characterization of the RPE membrane and most are lacking key properties such as the mechanical or the degradability, which are crucial features for the implant efficiency.

4.3.2. Animal models

After *in vitro* optimization and characterization of the RPE implants, many studies conducted animal experimentation to determine surgical feasibility, biocompatibility, implant integration and efficiency. The smaller animal model studied for RPE replacement is usually the rat. First, implantation tests in the subretinal space were often conducted in nude athymic rats (Crl:NIH-Foxn1^{rnu}) to test the feasibility of implantation, the survival of the graft and evaluate, in the case of stem cell-derived RPE, the risk of teratoma formation [73,80,94]. To test the therapeutic efficiency of the graft, the standard rat model is the Royal College of Surgeons (RCS) rat [158], characterized by an inherited retinal degeneration due to a mutation of a gene encoding the tyrosine kinase, MERTK [159]. Due to a defective phagocytosis of POS by the RPE, the degeneration starts two to three weeks after birth and the surgery is usually conducted on rats around 3–4 weeks old, when the degeneration is still incomplete [65,82,94] and up to 10 weeks old [64]. Graft efficiency can be evaluated by assessing visual acuity, using the optokinetic head movement reflex in rats after a visual stimulus, such as moving white stripes on a black background [82,94]. By analyzing the rats' response while reducing the stripes width, Ben M'Barek et al. showed that their implant allowed a sustained visual acuity, whereas untreated or sham-treated rats demonstrated a markedly reduced visual acuity after 3 months [94]. The functionality of the RPE cells can also be evaluated *in vitro* on the explants by measuring the phagocytosis capability of labelled POS by the RPE cells [82]. Histological assessment can also be conducted on explants to analyze photoreceptors survival, outer nuclear layer preservation and rod/cones ratio [65,82,94,99]. On top of graft efficiency, implantation in RCS rats also enables to evaluate the potential toxicity and immunogenicity of the graft [65,73,82,94], notably by implanting an acellular graft to solely study the impact of the material [89,99]. With a larger eye, making the implantation easier, rabbits have also been used for RPE transplantation. However, unlike the rats, there is no widespread rabbit model with inherited retinal degeneration, despite some advances by Kondo et al. [160,161]. Thus, to the best of our knowledge, all studies have been conducted in wild-type rabbit models such as New Zealand white rabbits [71,90,95], Chinchilla bastard rabbits [59,61,90] and Dutch-belted rabbits [61]. In these studies, the grafts have been implanted in the subretinal space to evaluate first the feasibility of the surgery and then their toxicity and immunogenicity along with the ONL disruption and the implanted RPE survival. However, since the rabbits do not present any retinal pathology, the graft efficiency could not be studied with these models. In future studies, a retinal degeneration could potentially be induced either by transgenic modification [160], by injection of sodium iodate [162–164], *N*-methyl-*N*-nitrosourea [163,164] or vitamin A dimers [165] or even by excessive visible light exposure [92]. Following encouraging results in small animal models and to test the graft at its clinical size, the use of larger animal models, with an eye size similar to humans, such as Yucatan minipigs [81], pigs [63,73] or non-human primates as the Cynomolgus monkeys [60,62,65,93] is necessary, notably to assess the surgical feasibility, the *in vivo* graft recovery and the immunogenicity. To test the graft efficiency in these larger animals, a disruption/degeneration of the oBRB needs to be induced prior to the implantation. This can notably be done by the use of a laser [73] for instance. In the specific case of AMD, a wider range of animal models are proposed including mice, rats, rabbits, pigs and non-human primate, all presenting several limitations [166].

4.3.3. Clinical translation

Thanks to successful pre-clinical evaluation on different animal models, several groups were able to translate their implants into clinics (see Table 4). To do so, they all first needed to report the obtention of the Good Manufacturing Practises (GMP) grade for their entire protocol, notably for the materials (polymer, coating proteins), the cell processing

Table 4
Clinical trials on the implantation of a RPE cell sheet.

Research center/ Company	Targeted disease	Material	Cell type	Implant size & Number of cells	Number of patients	Follow-up	Improvement of visual acuity	Clinical trial ID	Pre-clinical reports	Clinical reports
iSTEM institute	RP due to monogenic mutation	hAM (Biodegradable)	hESC-derived RPE	Around 100 μm thick	On-going	On-going	On-going	NCT03963154	[93,94]	Trial on-going
Regenerative Patch Technologies	Dry AMD	Parylene (Biodegradable)	hESC-derived RPE	3,5*6,25 mm^2, 6 μm thick & around 100,000 cells	15 (average of 78 yo)	1 year	ETDRS improved between 6 and 13 letters in a year	NCT02590692	[79–82]	[83–86]
Moorfields Eye Hospital NHS Foundation Trust & Pzifer	Wet and early dry AMD	PET (Non-biodegradable)	hESC-derived RPE	6*3 mm^2, 10 μm thick & around 100,000 cells	2 (above 60 yo)	1 year	ETDRS improved by 29 (Pat.1) and 21 (Pat.2) letters Reading speed improve from 1,7 to 82,8 words/min (Pat.1) and from 0 to 47,8 words/ min (Pat.2)	NCT01691261	[63]	[63]
National Eye Institute	Dry AMD	PLGA (Biodegradable)	hiPSC-derived RPE	4*2 mm^2, 10 μm thick & around 25,000 cells	On-going	On-going	On-going	NCT04339764	[73]	Trial on-going
RIKEN Center	Wet AMD	No substrate	hiPSC-derived RPE	1,3*3 mm^2 & around 50,000 cells	1 (77 yo)	4 years	VFQ-25 score improved from 48,8 to 58,3 in a year	UMIN000011929 (Japan)	[65]	[66,67]

Abbreviations: RP: retinitis pigmentosa; hAM: human amniotic membrane; PET: polyethylene terephthalate; PLGA: poly(L-lactic-co-glycolic acid); ETDRS: Early Treatment of Diabetic Retinopathy Severity Score; Pat: patient; VFQ-25: National Eye Institute Visual Functioning Questionnaire; yo: years old.

(differentiation, cryopreservation, culture) as well as the implant processing and delivery. The latter is particularly challenging, notably to implant the graft at the proper location and in the right position, without damaging it along the way. To improve the delivery success rate, several groups developed their own GMP-grade implantation devices [63,66,93,167,168].

To the best of our knowledge, 5 clinical trials have been registered, implanting a monolayer of RPE either on a polymeric substrate, or implanted as a cell sheet without substrate and their characteristics are presented in Table 4. Among those 5 clinical trials, three have reported results on their I/IIa stage [63,66,67,83–86]. Thanks to their own delivery device, the authors were able to deliver the graft at the proper location, with the RPE properly facing the ONL, thus demonstrating the feasibility of the surgery. Kashani et al. notably reported that, over 15 patients, 86.9% of the defect area was covered by the implant [83]. In those 3 reported clinical trials, they further showed that the implants do not damage the upper retinal structures, with a preservation of the photoreceptors. Several unexpected complications were still observed during the follow-up period, the most recurrent being apparition of haemorrhage. Indeed, over 15 patients, Kashani et al. reported systematic intra-retinal haemorrhage, and often subconjunctival (n = 12) and sub-retinal (n = 9) haemorrhages [83]. Da Cruz et al. also reported a retinal detachment in one patient, requiring additional surgery but without inducing graft damage [63]. Once implanted, the evaluation of the RPE cells behaviour is challenging, due to their location. The death, unrelated to the surgery, of a patient allowed Kashani et al. to explant and analyze the tissue, two years after the graft implantation [86]. At this timepoint, they reported that the implanted RPE survived, without any decrease in their pigmentation or expression of the typical markers and presented signs of POS phagocytosis. Even if stage I clinical trials involved patients with advanced retinal degeneration and considered as legally blind, the 3 studies reported a maintenance or an improvement of the visual acuity characterized by an improved ETDRS (Early Treatment of Diabetic Retinopathy Severity Score) or VFQ-25 (National Eye Institute Visual Functioning Questionnaire) score (see Table 4). Da Cruz et al. even reported increased reading speed for the two patients [63]. Those results are thus encouraging for the pursuits of the clinical trials on the implantation of RPE as a cell sheet in patients with less advanced retinal degeneration to evaluate the efficiency of the graft.

5. Conclusion and perspectives

Models of the oBRB have been developed for more than three decades, with an increasing complexity to mimic as closely as possible the native tissue. In the last years, the improvement of oBRB models has been further accelerated thanks to new technologies and techniques.

First, the discovery of new cell sources, including the primary cells and hESC-derived RPE cells, allowed to move away from the use of cell lines, such as the ARPE-19 cells, that do not recapitulate crucial features of the RPE cells (section 4.1.1.1). However, those particular cell types raised ethical concerns due to the need of donors or the production of human embryos (Sections 4.1.1.2 and 4.1.1.3.2). All these limitations were overcome with the emergence of the hiPSC-derived RPE cells (section 4.1.1.3.3). This powerful new cell type is a great tool for the development of *in vitro* models, notably by using cells derived from patients to study disease mechanisms and potential therapeutic strategies (section 4.2.2). Moreover, the hiPSC-derived RPE cells are today the best candidate for cellular therapy since, by using the patient's own cells or by using iPSC from cell banks, it is possible to avoid or minimize the risk of graft rejection (Sections 4.1.1.3.3 and 4.3).

Secondly, the development of new material processing techniques has enabled an increasing complexity in the design of the culture support. If, at the beginning, the models for *in vitro* applications were generally based on commercial Transwell inserts, they are now mostly designed using microfluidic chips, that allow both a 3D structuring of the tissue and the addition of flow (section 4.2.1). So far limited to the modelling of the RPE layer, *in vitro* models have recently started to include the choroidal compartment of the oBRB (section 4.2.3). First designed as a monolayered culture, the ECs-RPE co-culture models rapidly evolved using pattern vessels and, later, cell-encapsulating

hydrogels to form a more complex vessel network. Numerous benefits on the cellular behaviour are observed in the co-culture conditions, for both the RPE cells and the ECs, as detailed in section 4.2.3. The co-culture even extended to the addition of other cell types, such as fibroblasts, mesenchymal stem cells and pericytes, that also greatly participate to a better RPE cellular behaviour. It is thus our belief that future studies should incorporate multiple cell types to promote a proper maturation of the modelled oBRB, making the results even more relevant to translate to the native tissue (section 4.2.3).

The progress in material processing also participated in the development of more advanced membranes for RPE cellular therapy. Using either natural or synthetic materials, usually with a bio-functionalization, membranes have been synthesized using techniques such as electrospinning or bioprinting, notably to mimic the fibrous topography of the BM (section 4.3.3). In most studies, several optimization steps were conducted to improve the material in order to favor cellular adhesion and behaviour. Successfully implanted in various animal models (section 4.3.2), five implants reached the clinical trials, and the first reported studies showed promising results (section 4.3.3). To the best of our knowledge, the cell therapy models have all focused solely on the RPE layer. Taking into consideration the previously mentioned benefits of the co-culture, it could be interesting to implement co-culture with endothelial cells and/or support cells, to favor a better RPE behaviour in models for cellular therapy. This co-culture could take place only during the *in vitro* maturation of the RPE sheet or also be included in the graft for the implantation.

Thus, if the oBRB models have greatly evolved in the last years, recent studies pave the way for future further developments, on the cellular and material levels.

Ethics approval and consent to participate

This work requires no ethics approval nor consent to participate.

Declaration of competing interest

The authors declare no conflict of interest.

Acknowledgements

This work was supported by the “Fondation pour la Recherche Médicale” (FRM, France). The authors acknowledge the Ecole Polytechnique (Paris, France) and their AMX program for the PhD funding for C. Dujardin.

References

[1] F. O'Leary, M. Campbell, The blood–retina barrier in health and disease, FEBS J. 290 (2023) 878–891, https://doi.org/10.1111/febs.16330.
[2] J. Cehajic-Kapetanovic, M.S. Singh, E. Zrenner, R.E. MacLaren, Bioengineering strategies for restoring vision, Nat Biomed Eng 7 (2023) 387–404, https://doi.org/10.1038/s41551-021-00836-4.
[3] S.D. Schwartz, J.P. Hubschman, G. Heilwell, V. Franco-Cardenas, C.K. Pan, R. M. Ostrick, et al., Embryonic stem cell trials for macular degeneration: a preliminary report, Lancet 379 (2012) 713–720, https://doi.org/10.1016/S0140-6736(12)60028-2.
[4] S. Sugita, M. Mandai, Y. Hirami, S. Takagi, T. Maeda, M. Fujihara, et al., HLA-matched allogeneic IPS cells-derived rpe transplantation for macular degeneration, J. Clin. Med. 9 (2020) 1–18, https://doi.org/10.3390/jcm9072217.
[5] O. Strauss, The retinal pigment epithelium in visual function, Physiol. Rev. 85 (2005) 845–881, https://doi.org/10.1152/physrev.00021.2004.
[6] D.L. Nickla, J. Wallman, The multifunctional choroid, Prog. Retin. Eye Res. 29 (2010) 144–168, https://doi.org/10.1016/j.preteyeres.2009.12.002.
[7] G.T. Feke, H. Tagawa, D.M. Deupree, D.G. Goger, J. Sebag, J.J. Weiter, Blood flow in the normal human retina, Invest. Ophthalmol. Vis. Sci. 30 (1989) 58–65.
[8] M. Ferrara, G. Lugano, M.T. Sandinha, V.R. Kearns, B. Geraghty, D.H.W. Steel, Biomechanical properties of retina and choroid: a comprehensive review of techniques and translational relevance, Eye 35 (2021) 1818–1832, https://doi.org/10.1038/s41433-021-01437-w.
[9] M.J. Hogan, J. Alvarado, Studies on the human macula: IV. Aging changes in bruch's membrane, Arch. Ophthalmol. 77 (1967) 410–420, https://doi.org/10.1001/ARCHOPHT.1967.00980020412022.
[10] J.C. Booij, D.C. Baas, J. Beisekeeva, T.G.M.F. Gorgels, A.A.B. Bergen, The dynamic nature of Bruch's membrane, Prog. Retin. Eye Res. 29 (2010) 1–18, https://doi.org/10.1016/j.preteyeres.2009.08.003.
[11] R. Sparrrow J, P.Hamel C. Hicks D, The retinal pigment epithelium in health and disease, Curr. Mol. Med. 10 (2010) 802–823, https://doi.org/10.2174/156652410793937813.
[12] W.L. Wong, X. Su, X. Li, C.M.G. Cheung, R. Klein, C.Y. Cheng, et al., Global prevalence of age-related macular degeneration and disease burden projection for 2020 and 2040: a systematic review and meta-analysis, Lancet Global Health 2 (2014) 106–116, https://doi.org/10.1016/S2214-109X(13)70145-1.
[13] J. Ambati, B.J. Fowler, Mechanisms of age-related macular degeneration, Neuron 75 (2012) 26–39, https://doi.org/10.1016/j.neuron.2012.06.018.
[14] N.J.Y. Yeo, E.J.J. Chan, C. Cheung, Choroidal neovascularization: mechanisms of endothelial dysfunction, Front. Pharmacol. 10 (2019) 1363, https://doi.org/10.3389/fphar.2019.01363.
[15] R.J. Antcliff, J. Marshall, The pathogenesis of edema in diabetic maculopathy, Semin. Ophthalmol. 14 (1999) 223–232, https://doi.org/10.3109/08820539909069541.
[16] N. Bhagat, R.A. Grigorian, A. Tutela, M.A. Zarbin, Diabetic macular edema: pathogenesis and treatment, Surv. Ophthalmol. 54 (2009) 1–32, https://doi.org/10.1016/j.survophthal.2008.10.001.
[17] S.P. Daiger, L.S. Sullivan, S.J. Bowne, Genes and mutations causing retinitis pigmentosa, Clin. Genet. 84 (2013) 132–141, https://doi.org/10.1111/cge.12203.
[18] D.T. Hartong, E.L. Berson, T.P. Dryja, Retinitis Pigmentosa Prevalence and Inheritance Patterns, vol. 368, 2006.
[19] C. Hamel, Retinitis Pigmentosa on the portal for rare diseases and orphan drugs n. d. https://www.orpha.net/consor/cgi-bin/OC_Exp.php?Lng=EN&Expert=791. (Accessed 10 July 2023).
[20] D. Napoli, M. Biagioni, F. Billeri, B Di Marco, N. Orsini, E. Novelli, et al., Retinal pigment epithelium remodeling in mouse models of retinitis pigmentosa, Int. J. Mol. Sci. 22 (2021), https://doi.org/10.3390/ijms22105381.
[21] T.T. Duong, V. Vasireddy, P. Ramachandran, P.S. Herrera, L. Leo, C. Merkel, et al., Use of induced pluripotent stem cell models to probe the pathogenesis of Choroideremia and to develop a potential treatment, Stem Cell Res. 27 (2018) 140–150, https://doi.org/10.1016/j.scr.2018.01.009.
[22] M.E. Pennesi, D.G. Birch, J.L. Duncan, J. Bennett, A. Girach, Choroideremia: retinal degeneration with an unmet need, Retina 39 (2019) 2059–2069, https://doi.org/10.1097/IAE.0000000000002553.
[23] S. Hayasaka, T. Kodama, A. Ohira, Retinal risks of high-dose ornithine supplements: a review, Br. J. Nutr. 106 (2011) 801–811, https://doi.org/10.1017/S0007114511003291.
[24] O. Simell, K. Takki, Raised plasma-ornithine and gyrate atrophy of the choroid and retina, Lancet 301 (1973) 1031–1033, https://doi.org/10.1016/S0140-6736(73)90667-3.
[25] R. Montioli, I. Bellezza, M.A. Desbats, C. Borri Voltattorni, L. Salviati, B. Cellini, Deficit of human ornithine aminotransferase in gyrate atrophy: molecular, cellular, and clinical aspects, Biochim. Biophys. Acta, Proteins Proteomics 1869 (2021), 140555, https://doi.org/10.1016/j.bbapap.2020.140555.
[26] B. Kamaraj, R. Purohit, Mutational analysis of oculocutaneous albinism: a compact review, BioMed Res. Int. 2014 (2014), https://doi.org/10.1155/2014/905472.
[27] K. Grønskov, J. Ek, K. Brondum-Nielsen, Oculocutaneous albinism, Orphanet J. Rare Dis. 2 (2007) 43, https://doi.org/10.1186/1750-1172-2-43.
[28] R.A. Spritz, Molecular genetics of oculocutaneous albinism, Hum. Mol. Genet. 3 (1994) 1469–1475, https://doi.org/10.1093/HMG/3.SUPPL_1.1469.
[29] E. Piotter, M.E. McClements, R.E. Maclaren, Therapy approaches for stargardt disease, Biomolecules 11 (2021) 1179, https://doi.org/10.3390/biom11081179.
[30] L.C. Glazer, T.P. Dryja, Understanding the etiology of Stargardt's disease, Ophthalmol Clin North Am 15 (2002) 93–100, https://doi.org/10.1016/s0896-1549(01)00011-6.
[31] P. Tanna, R.W. Strauss, K. Fujinami, M. Michaelides, Stargardt disease: clinical features, molecular genetics, animal models and therapeutic options, Br. J. Ophthalmol. 101 (2017) 25–30, https://doi.org/10.1136/bjophthalmol-2016-308823.
[32] E.M. Stone, A.J. Lotery, F.L. Munier, E. Héon, B. Piguet, R.H. Guymer, et al., A single EFEMP1 mutation associated with both Malattia Leventinese and Doyne honeycomb retinal dystrophy, Nat. Genet. 22 (1999) 199–202.
[33] L.Y. Marmorstein, F.L. Munier, Y. Arsenijevic, D.F. Schorderet, P.J. Mclaughlin, D. Chung, et al., Aberrant accumulation of EFEMP1 underlies drusen formation in Malattia Leventinese and age-related macular degeneration, Proc. Natl. Acad. Sci. USA 99 (2002) 13067–13072, https://doi.org/10.1073/pnas.202491599.
[34] L.Y. Marmorstein, Association of EFEMP1 with malattia leventinese and age-related macular degeneration: a mini-review, Ophthalmic Genet. 25 (2004) 219–226, https://doi.org/10.1080/13816810490498305.
[35] J.D. Hulleman, Malattia leventinese/doyne honeycomb retinal dystrophy: similarities to age-related macular degeneration and potential therapies, Adv. Exp. Med. Biol. 854 (2016) 153–158, https://doi.org/10.1007/978-3-319-17121-0_21. Springer New York LLC.
[36] D.R.G. Christensen, F.E. Brown, A.J. Cree, J.A. Ratnayaka, A.J. Lotery, Sorsby fundus dystrophy – a review of pathology and disease mechanisms, Exp. Eye Res. 165 (2017) 35–46, https://doi.org/10.1016/j.exer.2017.08.014.

[37] A. Naylor, A. Hopkins, N. Hudson, M. Campbell, Tight junctions of the outer blood retina barrier, Int. J. Mol. Sci. 21 (2020), https://doi.org/10.3390/ijms21010211.

[38] A.W. Taylor, S. Hsu, T.F. Ng, The role of retinal pigment epithelial cells in regulation of macrophages/microglial cells in retinal immunobiology, Front. Immunol. 12 (2021), https://doi.org/10.3389/fimmu.2021.724601.

[39] A.W. Taylor, Ocular immune privilege, Eye 23 (2009) 1885–1889, https://doi.org/10.1038/eye.2008.382.

[40] K. Ishida, N. Panjwani, Z. Cao, J.W. Streilein, Participation of pigment epithelium in ocular immune privilege. 3. Epithelia cultured from iris, ciliary body, and retina suppress T-cell activation by partially non-overlapping mechanisms, Ocul. Immunol. Inflamm. 11 (2003) 91–105, https://doi.org/10.1076/ocii.11.2.91.15914.

[41] S. Sugita, Y. Kawazoe, A. Imai, Y. Usui, Y. Iwakura, K. Isoda, et al., Mature dendritic cell suppression by IL-1 receptor antagonist on retinal pigment epithelium cells, Invest. Ophthalmol. Vis. Sci. 54 (2013) 3240–3249, https://doi.org/10.1167/iovs.12-11483.

[42] V.L. Perez, R.R. Caspi, Immune mechanisms in inflammatory and degenerative eye disease, Trends Immunol. 36 (2015) 354–363, https://doi.org/10.1016/j.it.2015.04.003.

[43] K.V. Mohan, A. Mishra, A. Muniyasamy, P. Sinha, P. Sahu, A. Kesarwani, et al., Immunological consequences of compromised ocular immune privilege accelerate retinal degeneration in retinitis pigmentosa, Orphanet J. Rare Dis. 17 (2022), https://doi.org/10.1186/s13023-022-02528-x.

[44] F. O'Leary, M. Campbell, The blood–retina barrier in health and disease, FEBS J. 290 (2023) 878–891, https://doi.org/10.1111/febs.16330.

[45] P.V. Algvere Lennart Berglin Peter Gouras Yaohua Sheng, P.V. Algvere, L. Berglin, P. Gouras -Y Sheng, Transplantation of fetal retinal pigment epithelium in age-related macular degeneration with subfoveal neovascularization, Graefe's Arch. Clin. Exp. Ophthalmol. 232 (1994) 707–716.

[46] E.F. Moreira, H. Cai, T.H. Tezel, M.A. Fields, L.V. Del Priore, Reengineering human bruch's membrane increases rod outer segment phagocytosis by human retinal pigment epithelium, Transl Vis Sci Technol 4 (2015) 10, https://doi.org/10.1167/tvst.4.5.10.

[47] H. Cai, J. Gong, L.V. Del Priore, T.H. Tezel, M.A. Fields, Culturing of retinal pigment epithelial cells on an ex vivo model of aged human bruch's membrane, JoVE (2018), 75084, https://doi.org/10.3791/57084.

[48] J. Kim, J.Y. Park, J.S. Kong, H. Lee, J.Y. Won, D.W. Cho, Development of 3D printed bruch's membrane-mimetic substance for the maturation of retinal pigment epithelial cells, Int. J. Mol. Sci. 22 (2021) 1–17, https://doi.org/10.3390/ijms22031095.

[49] G. Maugeri, A.G. D'Amico, C. Gagliano, S. Saccone, C. Federico, S. Cavallaro, et al., VIP family members prevent outer blood retinal barrier damage in a model of diabetic macular edema, J. Cell. Physiol. 232 (2017) 1079–1085, https://doi.org/10.1002/jcp.25510.

[50] G. Maugeri, A.G. D'Amico, D.M. Rasà, V. La Cognata, S. Saccone, C. Federico, et al., Nicotine promotes blood retinal barrier damage in a model of human diabetic macular edema, Toxicol. Vitro 44 (2017) 182–189, https://doi.org/10.1016/j.tiv.2017.07.003.

[51] G. Maugeri, A.G. D'Amico, D.M. Rasà, V. La Cognata, S. Saccone, C. Federico, et al., Caffeine prevents blood retinal barrier damage in a model, in vitro, of diabetic macular edema, J. Cell. Biochem. 118 (2017) 2371–2379, https://doi.org/10.1002/jcb.25899.

[52] A.G. D'Amico, G. Maugeri, D. Rasà, C. Federico, S. Saccone, F. Lazzara, et al., NAP modulates hyperglycemic–inflammatory event of diabetic retina by counteracting outer blood retinal barrier damage, J. Cell. Physiol. 234 (2019) 5230–5240, https://doi.org/10.1002/jcp.27331.

[53] Z.B. Doğanlar, O. Doğanlar, K. Kurtdere, H. Güçlü, T. Chasan, E. Turgut, Melatonin prevents blood-retinal barrier breakdown and mitochondrial dysfunction in high glucose and hypoxia-induced in vitro diabetic macular edema model, Toxicol. Vitro 75 (2021), 105191, https://doi.org/10.1016/j.tiv.2021.105191.

[54] E. Mannermaa, M. Reinisalo, V.P. Ranta, K.S. Vellonen, H. Kokki, A. Saarikko, et al., Filter-cultured ARPE-19 cells as outer blood-retinal barrier model, Eur. J. Pharmaceut. Sci. 40 (2010) 289–296, https://doi.org/10.1016/j.ejps.2010.04.001.

[55] R.S. Kadam, R.I. Scheinman, U.B. Kompella, Pigmented-MDCK (P-MDCK) cell line with tunable melanin expression: an in vitro model for the outer blood-retinal barrier, Mol. Pharm. 9 (2012) 3228–3235, https://doi.org/10.1021/mp300305f.

[56] S. Peng, G. Gan, C. Qiu, M. Zhong, H. An, R.A. Adelman, et al., Engineering a blood-retinal barrier with human embryonic stem cell-derived retinal pigment epithelium: transcriptome and functional analysis, Stem Cells Transl Med 2 (2013) 534–544, https://doi.org/10.5966/sctm.2012-0134.

[57] A. Maminishkis, S. Chen, S. Jalickee, T. Banzon, G. Shi, F.E. Wang, et al., Confluent monolayers of cultured human fetal retinal pigment epithelium exhibit morphology and physiology of native tissue, Invest. Ophthalmol. Vis. Sci. 47 (2006) 3612–3624, https://doi.org/10.1167/iovs.05-1622.

[58] A. George, R. Sharma, T. Pfister, M. Abu-Asab, N. Hotaling, D. Bose, et al., In vitro disease modeling of oculocutaneous albinism type 1 and 2 using human induced pluripotent stem cell-derived retinal pigment epithelium, Stem Cell Rep. 17 (2022) 173–186, https://doi.org/10.1016/j.stemcr.2021.11.016.

[59] B.V. Stanzel, Z. Liu, S. Somboonthanakij, W. Wongsawad, R. Brinken, N. Eter, et al., Human RPE stem cells grown into polarized RPE monolayers on a polyester matrix are maintained after grafting into rabbit subretinal space, Stem Cell Rep. 2 (2014) 64–77, https://doi.org/10.1016/j.stemcr.2013.11.005.

[60] Z. Liu, B.H. Parikh, Q.S.W. Tan, D.S.L. Wong, K.H. Ong, W. Yu, et al., Surgical transplantation of human RPE stem cell-derived RPE monolayers into non-human primates with immunosuppression, Stem Cell Rep. 16 (2021) 237–251, https://doi.org/10.1016/j.stemcr.2020.12.007.

[61] T. Ilmarinen, F. Thieltges, H. Hongisto, K. Juuti-Uusitalo, A. Koistinen, K. Kaarniranta, et al., Survival and functionality of xeno-free human embryonic stem cell–derived retinal pigment epithelial cells on polyester substrate after transplantation in rabbits, Acta Ophthalmol. 97 (2019) e688–e699, https://doi.org/10.1111/aos.14004.

[62] Z. Liu, T. Ilmarinen, G.S.W. Tan, H. Hongisto, E.Y.M. Wong, A.S.H. Tsai, et al., Submacular integration of hESC-RPE monolayer xenografts in a surgical non-human primate model, Stem Cell Res. Ther. 12 (2021) 1–16, https://doi.org/10.1186/s13287-021-02395-6.

[63] L. Da Cruz, K. Fynes, O. Georgiadis, J. Kerby, Y.H. Luo, A. Ahmado, et al., Phase 1 clinical study of an embryonic stem cell-derived retinal pigment epithelium patch in age-related macular degeneration, Nat. Biotechnol. 36 (2018) 328–337, https://doi.org/10.1038/nbt.4114.

[64] S. Soroushzadeh, F. Karamali, E. Masaeli, A. Atefi, M.H. Nasr Esfahani, Scaffold free retinal pigment epithelium sheet engineering using modified alginate-RGD hydrogel, J. Biosci. Bioeng. 133 (2022) 579–586, https://doi.org/10.1016/j.jbiosc.2022.02.002.

[65] H. Kamao, M. Mandai, S. Okamoto, N. Sakai, A. Suga, S. Sugita, et al., Characterization of human induced pluripotent stem cell-derived retinal pigment epithelium cell sheets aiming for clinical application, Stem Cell Rep. 2 (2014) 205–218, https://doi.org/10.1016/j.stemcr.2013.12.007.

[66] M. Mandai, A. Watanabe, Y. Kurimoto, Y. Hirami, C. Morinaga, T. Daimon, et al., Autologous induced stem-cell–derived retinal cells for macular degeneration, N. Engl. J. Med. 376 (2017) 1038–1046, https://doi.org/10.1056/nejmoa1608368.

[67] S. Takagi, M. Mandai, K. Gocho, Y. Hirami, M. Yamamoto, M. Fujihara, et al., Evaluation of transplanted autologous induced pluripotent stem cell-derived retinal pigment epithelium in exudative age-related macular degeneration, Ophthalmol Retina 3 (2019) 850–859, https://doi.org/10.1016/j.oret.2019.04.021.

[68] M. Nishida, Y. Tanaka, Y. Tanaka, S. Amaya, N. Tanaka, H. Uyama, et al., Human iPS cell derived RPE strips for secure delivery of graft cells at a target place with minimal surgical invasion, Sci. Rep. 11 (2021), 21421, https://doi.org/10.1038/s41598-021-00703-x.

[69] G. Thumann, A. Viethen, A. Gaebler, P. Walter, S. Kaempf, S. Johnen, et al., The in vitro and in vivo behaviour of retinal pigment epithelial cells cultured on ultrathin collagen membranes, Biomaterials 30 (2009) 287–294, https://doi.org/10.1016/j.biomaterials.2008.09.039.

[70] A. Subrizi, H. Hiidenmaa, T. Ilmarinen, S. Nymark, P. Dubruel, H. Uusitalo, et al., Generation of hESC-derived retinal pigment epithelium on biopolymer coated polyimide membranes, Biomaterials 33 (2012) 8047–8054, https://doi.org/10.1016/j.biomaterials.2012.07.033.

[71] T. Ilmarinen, H. Hiidenmaa, P. Kööbi, S. Nymark, A. Sorkio, J.H. Wang, et al., Ultrathin polyimide membrane as cell carrier for subretinal transplantation of human embryonic stem cell derived retinal pigment epithelium, PLoS One 10 (2015), e0143669, https://doi.org/10.1371/journal.pone.0143669.

[72] G.G. Giordano, R.C. Thomson, S.L. Ishaug, A.G. Mikos, S. Cumber, C.A. Garcia, et al., Retinal pigment epithelium cells cultured on synthetic biodegradable polymers, J. Biomed. Mater. Res. 34 (1997) 87–93, https://doi.org/10.1002/(SICI)1097-4636(199701)34:1<87::AID-JBM12>3.0.CO;2-M.

[73] R. Sharma, V. Khristov, A. Rising, B. Shekhar Jha, R. Dejene, N. Hotaling, et al., Clinical-grade stem cell-derived retinal pigment epithelium patch rescues retinal degeneration in rodents and pigs, Sci. Transl. Med. 11 (2019) 5580, https://doi.org/10.1126/scitranslmed.aat5580.

[74] S. Singh, S. Woerly, B.J. Mclaughlin, Natural and artificial substrates for retinal pigment epithelial monolayer transplantation, Biomaterials 22 (2001) 3337–3343, https://doi.org/10.1016/S0142-9612(01)00171-5.

[75] A. Tezcaner, K. Bugra, V. Hasirci, Retinal pigment epithelium cell culture on surface modified poly(hydroxybutyrate-co-hydroxyvalerate) thin films, Biomaterials 24 (2003) 4573–4583, https://doi.org/10.1016/S0142-9612(03)00302-8.

[76] Y. Krishna, C. Sheridan, D. Kent, V. Kearns, I. Grierson, R. Williams, Expanded polytetrafluoroethylene as a substrate for retinal pigment epithelial cell growth and transplantation in age-related macular degeneration, Br. J. Ophthalmol. 95 (2011) 569–573, https://doi.org/10.1136/bjo.2009.169953.

[77] Y. Krishna, C.M. Sheridan, D.L. Kent, I. Grierson, R.L. Williams, Polydimethylsiloxane as a substrate for retinal pigment epithelial cell growth, J. Biomed. Mater. Res. 80 (2007) 669–678, https://doi.org/10.1002/jbm.a.30953.

[78] V.R. Kearns, J. Tasker, Akhtar R. Zhuola, A. Bachhuka, K. Vasilev, et al., The formation of a functional retinal pigment epithelium occurs on porous polytetrafluoroethylene substrates independently of the surface chemistry, J. Mater. Sci. Mater. Med. 28 (2017) 1–14, https://doi.org/10.1007/s10856-017-5926-3.

[79] B. Lu, D. Zhu, D. Hinton, M.S. Humayun, Y.C. Tai, Mesh-supported submicron parylene-C membranes for culturing retinal pigment epithelial cells, Biomed. Microdevices 14 (2012) 659–667, https://doi.org/10.1007/s10544-012-9645-8.

[80] B. Diniz, P. Thomas, B. Thomas, R. Ribeiro, Y. Hu, R. Brant, et al., Subretinal implantation of retinal pigment epithelial cells derived from human embryonic stem cells: improved survival when implanted as a monolayer, Invest. Ophthalmol. Vis. Sci. 54 (2013) 5087–5096, https://doi.org/10.1167/iovs.12-11239.

[81] M.J. Koss, P. Falabella, F.R. Stefanini, M. Pfister, B.B. Thomas, A.H. Kashani, et al., Subretinal implantation of a monolayer of human embryonic stem cell-derived retinal pigment epithelium: a feasibility and safety study in Yucatán minipigs, Graefe's Arch. Clin. Exp. Ophthalmol. 254 (2016) 1553–1565, https://doi.org/10.1007/s00417-016-3386-y.

[82] B.B. Thomas, D. Zhu, L. Zhang, P.B. Thomas, Y. Hu, H. Nazari, et al., Survival and functionality of hESC-derived retinal pigment epithelium cells cultured as a monolayer on polymer substrates transplanted in RCS rats, Invest. Ophthalmol. Vis. Sci. 57 (2016) 2877–2887, https://doi.org/10.1167/iovs.16-19238.

[83] A.H. Kashani, J. Uang, M. Mert, F. Rahhal, C. Chan, R.L. Avery, et al., Surgical method for implantation of a biosynthetic retinal pigment epithelium monolayer for geographic atrophy: experience from a phase 1/2a study, Ophthalmol Retina 4 (2020) 264–273, https://doi.org/10.1016/j.oret.2019.09.017.

[84] A.H. Kashani, J.S. Lebkowski, F.M. Rahhal, R.L. Avery, H. Salehi-Had, W. Dang, et al., A bioengineered retinal pigment epithelial monolayer for advanced, dry age-related macular degeneration, Sci. Transl. Med. 10 (2018), eaao4097, https://doi.org/10.1126/scitranslmed.aao4097.

[85] A.H. Kashani, J.S. Lebkowski, F.M. Rahhal, R.L. Avery, H. Salehi-Had, S. Chen, et al., One-year follow-up in a phase 1/2a clinical trial of an allogeneic rpe cell bioengineered implant for advanced dry age-related macular degeneration, Transl Vis Sci Technol 10 (2021) 13, https://doi.org/10.1167/TVST.10.10.13.

[86] A.H. Kashani, J.S. Lebkowski, D.R. Hinton, D. Zhu, M.A. Faynus, S. Chen, et al., Survival of an HLA-mismatched, bioengineered RPE implant in dry age-related macular degeneration, Stem Cell Rep. 17 (2022) 448–458, https://doi.org/10.1016/j.stemcr.2022.01.001.

[87] M.T. Calejo, A. Haapala, H. Skottman, M. Kellomäki, Porous polybutylene succinate films enabling adhesion of human embryonic stem cell-derived retinal pigment epithelial cells (hESC-RPE), Eur. Polym. J. 118 (2019) 78–87, https://doi.org/10.1016/j.eurpolymj.2019.05.041.

[88] P.H. Warnke, M. Alamein, S. Skabo, S. Stephens, R. Bourke, P. Heiner, et al., Primordium of an artificial Bruch's membrane made of nanofibers for engineering of retinal pigment epithelium cell monolayers, Acta Biomater. 9 (2013) 9414–9422, https://doi.org/10.1016/j.actbio.2013.07.029.

[89] D.C. Surrao, U. Greferath, Y.Q. Chau, S.J. Skabo, M. Huynh, K.J. Shelat, et al., Design, development and characterization of synthetic Bruch's membranes, Acta Biomater. 64 (2017) 357–376, https://doi.org/10.1016/j.actbio.2017.09.032.

[90] Z. Liu, N. Yu, F.G. Holz, F. Yang, B.V. Stanzel, Enhancement of retinal pigment epithelial culture characteristics and subretinal space tolerance of scaffolds with 200 nm fiber topography, Biomaterials 35 (2014) 2837–2850, https://doi.org/10.1016/j.biomaterials.2013.12.069.

[91] S.Y. Chan, B.Q.Y. Chan, Z. Liu, B.H. Parikh, K. Zhang, Q. Lin, et al., Electrospun pectin-polyhydroxybutyrate nanofibers for retinal tissue engineering, ACS Omega 2 (2017) 8959–8968, https://doi.org/10.1021/acsomega.7b01604.

[92] S. Wang, S. Lin, B. Xue, C. Wang, N. Yan, Y. Guan, et al., Bruch's-Mimetic nanofibrous membranes functionalized with the integrin-binding peptides as a promising approach for human retinal pigment epithelium cell transplantation, Molecules 27 (2022) 1429, https://doi.org/10.3390/molecules27041429.

[93] K. Ben M'Barek, S. Bertin, E. Brazhnikova, C. Jaillard, W. Habeler, A. Plancheron, et al., Clinical-grade production and safe delivery of human ESC derived RPE sheets in primates and rodents, Biomaterials 230 (2020), 119603, https://doi.org/10.1016/j.biomaterials.2019.119603.

[94] K. Ben M'barek, W. Habeler, A. Plancheron, M. Jarraya, F. Regent, A. Terray, et al., Human ESC-derived retinal epithelial cell sheets potentiate rescue of photoreceptor cell loss in rats with retinal degeneration, Sci. Transl. Med. 9 (2017) 7471, https://doi.org/10.1126/scitranslmed.aai7471.

[95] S. Zhang, K. Ye, G. Gao, X. Song, P. Xu, J. Zeng, et al., Amniotic membrane enhances the characteristics and function of stem cell-derived retinal pigment epithelium sheets by inhibiting the epithelial–mesenchymal transition, Acta Biomater. 151 (2022) 183–196, https://doi.org/10.1016/j.actbio.2022.07.064.

[96] E. Majidnia, M. Ahmadian, H. Salehi, N. Amirpour, Development of an electrospun poly(ε-caprolactone)/collagen-based human amniotic membrane powder scaffold for culturing retinal pigment epithelial cells, Sci. Rep. 12 (2022) 6469, https://doi.org/10.1038/s41598-022-09957-5.

[97] A.M.A. Shadforth, S. Suzuki, C. Theodoropoulos, N.A. Richardson, T.V. Chirila, D. G. Harkin, A Bruch's membrane substitute fabricated from silk fibroin supports the function of retinal pigment epithelial cells in vitro, J Tissue Eng Regen Med 11 (2017) 1915–1924, https://doi.org/10.1002/term.2089.

[98] C.A. Galloway, S. Dalvi, A.M.A. Shadforth, S. Suzuki, M. Wilson, D. Kuai, et al., Characterization of human iPSC-RPE on a prosthetic bruch's membrane manufactured from silk fibroin, Invest. Ophthalmol. Vis. Sci. 59 (2018) 2792–2800, https://doi.org/10.1167/iovs.17-23157.

[99] S. Suzuki, A.M.A. Shadforth, S. McLenachan, D. Zhang, S.C. Chen, J. Walshe, et al., Optimization of silk fibroin membranes for retinal implantation, Mater. Sci. Eng. C 105 (2019), 110131, https://doi.org/10.1016/j.msec.2019.110131.

[100] M.E. Hartnett, A. Lappas, D. Darland, J.R. McColm, S. Lovejoy, P.A. D'Amore, Retinal pigment epithelium and endothelial cell interaction causes retinal pigment epithelial barrier dysfunction via a soluble VEGF-dependent mechanism, Exp. Eye Res. 77 (2003) 593–599, https://doi.org/10.1016/S0014-4835(03)00189-1.

[101] R.D. Hamilton, A.J. Foss, L. Leach, Establishment of a human in vitro model of the outer blood-retinal barrier, J. Anat. 211 (2007) 707–716, https://doi.org/10.1111/j.1469-7580.2007.00812.x.

[102] C. Spencer, S. Abend, K.J. McHugh, M. Saint-Geniez, Identification of a synergistic interaction between endothelial cells and retinal pigment epithelium, J. Cell Mol. Med. 21 (2017) 2542–2552, https://doi.org/10.1111/jcmm.13175.

[103] I. Benedicto, G.L. Lehmann, M. Ginsberg, D.J. Nolan, R. Bareja, O. Elemento, et al., Concerted regulation of retinal pigment epithelium basement membrane and barrier function by angiocrine factors, Nat. Commun. 8 (2017), 15374, https://doi.org/10.1038/ncomms15374.

[104] R. Kumar, S. Harris-Hooker, R. Kumar, G. Sanford, Co-culture of retinal and endothelial cells results in the modulation of genes critical to retinal neovascularization, Vasc. Cell 3 (2011) 1–15, https://doi.org/10.1186/2045-824X-3-27.

[105] M.T. Calejo, J. Saari, H. Vuorenpää, E. Vuorimaa-Laukkanen, P. Kallio, K. Aalto-Setälä, et al., Co-culture of human induced pluripotent stem cell-derived retinal pigment epithelial cells and endothelial cells on double collagen-coated honeycomb films, Acta Biomater. 101 (2020) 327–343, https://doi.org/10.1016/j.actbio.2019.11.002.

[106] L.J. Chen, S. Ito, H. Kai, K. Nagamine, N. Nagai, M. Nishizawa, et al., Microfluidic co-cultures of retinal pigment epithelial cells and vascular endothelial cells to investigate choroidal angiogenesis, Sci. Rep. 7 (2017) 1–9, https://doi.org/10.1038/s41598-017-03788-5.

[107] L.J. Chen, B. Raut, N. Nagai, T. Abe, H. Kaji, Prototyping a versatile two-layer multi-channel microfluidic device for direct-contact cell-vessel co-culture, Micromachines 11 (2020) 79, https://doi.org/10.3390/mi11010079.

[108] Y.B. Arik, W. Buijsman, J. Loessberg-Zahl, C. Cuartas-Vélez, C. Veenstra, S. Logtenberg, et al., Microfluidic organ-on-a-chip model of the outer blood-retinal barrier with clinically relevant read-outs for tissue permeability and vascular structure, Lab Chip 21 (2021) 272–283, https://doi.org/10.1039/d0lc00639d.

[109] A. Komez, E.T. Baran, U. Erdem, N. Hasirci, V. Hasirci, Construction of a patterned hydrogel—fibrous mat bilayer structure to mimic choroid and Bruch's membrane layers of retina, J. Biomed. Mater. Res. 104 (2016) 2166–2177, https://doi.org/10.1002/jbm.a.35756.

[110] M. Chung, S. Lee, B.J. Lee, K. Son, N.L. Jeon, J.H. Kim, Wet-AMD on a chip: modeling outer blood-retinal barrier in vitro, Adv Healthc Mater 7 (2018), 1700028, https://doi.org/10.1002/adhm.201700028.

[111] J. Paek, S.E. Park, Q. Lu, K.T. Park, M. Cho, J.M. Oh, et al., Microphysiological engineering of self-assembled and perfusable microvascular beds for the production of vascularized three-dimensional human microtissues, ACS Nano 13 (2019) 7627–7643, https://doi.org/10.1021/acsnano.9b00686.

[112] K.V. Manian, C.A. Galloway, S. Dalvi, A.A. Emanuel, J.A. Mereness, W. Black, et al., 3D iPSC modeling of the retinal pigment epithelium-choriocapillaris complex identifies factors involved in the pathology of macular degeneration, Cell Stem Cell 28 (2021) 846–862.e8, https://doi.org/10.1016/j.stem.2021.02.006.

[113] M.J. Song, R. Quinn, E. Nguyen, C. Hampton, R. Sharma, T.S. Park, et al., Bioprinted 3D outer retina barrier uncovers RPE-dependent choroidal phenotype in advanced macular degeneration, Nat. Methods 20 (2023) 149–161, https://doi.org/10.1038/s41592-022-01701-1.

[114] J. Mannagh, D.V. Arya, A.R. Irvine, Tissue culture of human retinal pigment epithelium, Invest. Ophthalmol. Vis. Sci. 12 (1973) 52–64.

[115] A.H. Fronk, E. Vargis, Methods for culturing retinal pigment epithelial cells: a review of current protocols and future recommendations, J. Tissue Eng. 7 (2016), 2041731416650838, https://doi.org/10.1177/2041731416650838.

[116] K.C. Dunn, A.E. Aotaki-Keen, F.R. Putkey, L.M. Hjelmeland, ARPE-19, A human retinal pigment epithelial cell line with differentiated properties, Exp. Eye Res. 62 (1996) 155–170, https://doi.org/10.1006/EXER.1996.0020.

[117] A.E. Davies, R.L. Williams, G. Lugano, S.R. Pop, V.R. Kearns, In vitro and computational modelling of drug delivery across the outer blood–retinal barrier, Interface Focus 10 (2020), 20190132, https://doi.org/10.1098/rsfs.2019.0132.

[118] V. Kearns, A. Mistry, S. Mason, Y. Krishna, C. Sheridan, R. Short, et al., Plasma polymer coatings to aid retinal pigment epithelial growth for transplantation in the treatment of age related macular degeneration, J. Mater. Sci. Mater. Med. 23 (2012) 2013–2021, https://doi.org/10.1007/s10856-012-4675-6.

[119] L. Hellinen, M. Hagström, H. Knuutila, M. Ruponen, A. Urtti, M. Reinisalo, Characterization of artificially re-pigmented ARPE-19 retinal pigment epithelial cell model, Sci. Rep. 9 (2019) 1–10, https://doi.org/10.1038/s41598-019-50324-8.

[120] R.H. Quinn, S.S. Miller, Ion transport mechanisms in native human retinal pigment epithelium, Invest. Ophthalmol. Vis. Sci. 33 (1992) 3513–3527.

[121] A.A. Davis, P.S. Bernstein, D. Bok, J. Turner, M. Nachtigal, R.C. Hunt, A human retinal pigment epithelial cell line that retains epithelial characteristics after prolonged culture, Invest. Ophthalmol. Vis. Sci. 36 (1995) 955–964.

[122] M. La Cour, H. Lin, E. Kenyon, S.S. Millerf, Lactate transport in freshly isolated human fetal retinal pigment epithelium, Invest. Ophthalmol. Vis. Sci. 35 (1994) 434–442.

[123] S. Mennel, S. Peter, C.H. Meyer, G. Thumann, Effect of photodynamic therapy on the function of the outer blood-retinal barrier in an in vitro model, Graefe's Arch. Clin. Exp. Ophthalmol. 244 (2006) 1015–1021, https://doi.org/10.1007/s00417-005-0237-7.

[124] D. Kent, C.M. Sheridan, H.A. Tomkinson, S.J. White, P. Hiscott, Lugang, et al., Edible mushroom (Agaricus bisporus) lectin inhibits human retinal pigment epithelial cell proliferation in vitro, Wound Repair Regen. 11 (2003) 285–291, https://doi.org/10.1046/j.1524-475X.2003.11408.x.

[125] E. Bertolotti, A. Neri, M. Camparini, C. Macaluso, V. Marigo, Stem cells as source for retinal pigment epithelium transplantation, Prog. Retin. Eye Res. 42 (2014) 130–144, https://doi.org/10.1016/j.preteyeres.2014.06.002.

[126] L.L. Leach, D.O. Clegg, Concise review: making stem cells retinal: methods for deriving retinal pigment epithelium and implications for patients with ocular disease, Stem Cell. 33 (2015) 2363–2373, https://doi.org/10.1002/stem.2010.

[127] S. Dehghan, R. Mirshahi, A. Shoae-Hassani, M. Naseripour, Human-induced pluripotent stem cells-derived retinal pigmented epithelium, a new horizon for cells-based therapies for age-related macular degeneration, Stem Cell Res. Ther. 13 (2022) 217, https://doi.org/10.1186/s13287-022-02894-0.
[128] E. Salero, T.A. Blenkinsop, B. Corneo, A. Harris, D. Rabin, J.H. Stern, et al., Adult human RPE can be activated into a multipotent stem cell that produces mesenchymal derivatives, Cell Stem Cell 10 (2012) 88–95, https://doi.org/10.1016/j.stem.2011.11.018.
[129] J.S. Saini, B. Corneo, J.D. Miller, T.R. Kiehl, Q. Wang, N.C. Boles, et al., Nicotinamide ameliorates disease phenotypes in a human iPSC model of age-related macular degeneration, Cell Stem Cell 20 (2017) 635–647.e7, https://doi.org/10.1016/j.stem.2016.12.015.
[130] J.A. Thomson, Embryonic stem cell lines derived from human blastocysts, Science 1998 (282) (1979) 1145–1147, https://doi.org/10.1126/science.282.5391.1145.
[131] I. Klimanskaya, J. Hipp, K.A. Rezai, M. West, A. Atala, R. Lanza, Derivation and comparative assessment of retinal pigment epithelium from human embryonic stem cells using transcriptomics, Clon Stem Cell 6 (2004) 217–245, https://doi.org/10.1089/clo.2004.6.217.
[132] A.T. Rogojina, W.E. Orr, B.K. Song, E.E. Geisert, Comparing the use of Affymetrix to spotted oligonucleotide microarrays using two retinal pigment epithelium cell lines, Mol. Vis. 9 (2003) 482.
[133] C. Flahou, T. Morishima, H. Takizawa, N. Sugimoto, Fit-for-all iPSC-derived cell therapies and their evaluation in humanized mice with NK cell immunity, Front. Immunol. 12 (2021) 1071, https://doi.org/10.3389/fimmu.2021.662360.
[134] K. Takahashi, K. Tanabe, M. Ohnuki, M. Narita, T. Ichisaka, K. Tomoda, et al., Induction of pluripotent stem cells from adult human fibroblasts by defined factors, Cell 131 (2007) 861–872, https://doi.org/10.1016/J.CELL.2007.11.019.
[135] Y. Hirami, F. Osakada, K. Takahashi, K. Okita, S. Yamanaka, H. Ikeda, et al., Generation of retinal cells from mouse and human induced pluripotent stem cells, Neurosci. Lett. 458 (2009) 126–131, https://doi.org/10.1016/J.NEULET.2009.04.035.
[136] D.E. Buchholz, S.T. Hikita, T.J. Rowland, A.M. Friedrich, C.R. Hinman, L. V. Johnson, et al., Derivation of functional retinal pigmented epithelium from induced pluripotent stem cells, Stem Cell. 27 (2009) 2427–2434, https://doi.org/10.1002/STEM.189.
[137] J.S. Meyer, S.E. Howden, K.A. Wallace, A.D. Verhoeven, L.S. Wright, E. E. Capowski, et al., Optic vesicle-like structures derived from human pluripotent stem cells facilitate a customized approach to retinal disease treatment, Stem Cell. 29 (2011) 1206–1218, https://doi.org/10.1002/stem.674.
[138] E. Matsumoto, N. Koide, H. Hanzawa, M. Kiyama, M. Ohta, J. Kuwabara, et al., Fabricating retinal pigment epithelial cell sheets derived from human induced pluripotent stem cells in an automated closed culture system for regenerative medicine, PLoS One 14 (2019), e0212369, https://doi.org/10.1371/journal.pone.0212369.
[139] D. Dorjsuren, R.T. Eastman, M.J. Song, A. Yasgar, Y. Chen, K. Bharti, et al., A platform of assays for the discovery of anti-Zika small-molecules with activity in a 3D-bioprinted outer-blood-retina model, PLoS One 17 (2022), e0261821, https://doi.org/10.1371/JOURNAL.PONE.0261821.
[140] J. Gong, H. Cai, S. Noggle, D. Paull, L.J. Rizzolo, L.V. Del Priore, et al., Stem cell-derived retinal pigment epithelium from patients with age-related macular degeneration exhibit reduced metabolism and matrix interactions, Stem Cells Transl Med 9 (2020) 364–376, https://doi.org/10.1002/sctm.19-0321.
[141] J.M. Skeie, R.F. Mullins, Elastin-mediated choroidal endothelial cell migration: possible role in age-related macular degeneration, Invest. Ophthalmol. Vis. Sci. 49 (2008) 5574–5580, https://doi.org/10.1167/iovs.08-1984.
[142] A.C. Browning, T. Gray, W.M. Amoaku, Isolation, culture, and characterisation of human macular inner choroidal microvascular endothelial cells, Br. J. Ophthalmol. 89 (2005) 1343–1347, https://doi.org/10.1136/bjo.2004.063602.
[143] M.A. Loeven, J.J. van Gemst, C.M.S. Schophuizen, V. Tilakaratna, L.P. van Den Heuvel, A.J. Day, et al., A novel choroidal endothelial cell line has a decreased affinity for the age-related macular degeneration– associated complement factor h variant 402h, Invest. Ophthalmol. Vis. Sci. 59 (2018) 722–730, https://doi.org/10.1167/iovs.IOVS-17-22893.
[144] J.C. Giacalone, M.J. Miller, G. Workalemahu, A.J. Reutzel, D. Ochoa, S. S. Whitmore, et al., Generation of an immortalized human choroid endothelial cell line (iChEC-1) using an endothelial cell specific promoter, Microvasc. Res. 123 (2019) 50–57, https://doi.org/10.1016/j.mvr.2018.12.002.
[145] A. Dellaquila, C. Le Bao, D. Letourneur, T. Simon-Yarza, In vitro strategies to vascularize 3D physiologically relevant models, Adv. Sci. 8 (2021), 2100798, https://doi.org/10.1002/advs.202100798.
[146] A.C. Browning, E.P. Halligan, E.A. Stewart, D.C. Swan, R. Dove, G. J. Samaranayake, et al., Comparative gene expression profiling of human umbilical vein endothelial cells and ocular vascular endothelial cells, Br. J. Ophthalmol. 96 (2012) 128–132, https://doi.org/10.1136/bjophthalmol-2011-300572.
[147] C.A. Galloway, S. Dalvi, S.S.C. Hung, L.A. MacDonald, L.R. Latchney, R.C. B. Wong, et al., Drusen in patient-derived hiPSC-RPE models of macular dystrophies, Proc. Natl. Acad. Sci. U. S. A. 114 (2017) E8214–E8223, https://doi.org/10.1073/pnas.1710430114.
[148] M.T. Calejo, J. Saari, H. Vuorenpää, E. Vuorimaa-Laukkanen, P. Kallio, K. Aalto-Setälä, et al., Co-culture of human induced pluripotent stem cell-derived retinal pigment epithelial cells and endothelial cells on double collagen-coated honeycomb films, Acta Biomater. 101 (2020) 327–343, https://doi.org/10.1016/j.actbio.2019.11.002.
[149] S. Lee, S. Kim, J.S. Jeon, Microfluidic outer blood–retinal barrier model for inducing wet age-related macular degeneration by hypoxic stress, Lab Chip 22 (2022) 4359–4368, https://doi.org/10.1039/D2LC00672C.
[150] J. Kim, J.S. Kong, H. Kim, W. Han, J.Y. Won, D.-W. Cho, et al., Maturation and protection effect of retinal tissue-derived bioink for 3D cell printing technology, Pharmaceutics 13 (2021) 934, https://doi.org/10.3390/pharmaceutics13070934.
[151] R. Sharma, D. Bose, A. Maminishkis, K. Bharti, Retinal pigment epithelium replacement therapy for age-related macular degeneration: are we there yet? Annual Review of Pharmacology and Toxicology Annu Rev Pharmacol Toxicol 60 (2020 2019) 553–572, https://doi.org/10.1146/annurev-pharmtox-010919.
[152] M.H. Goldbaum, K. Madden, A new perspective on Bruch's membrane and the retinal pigment epithelium, Br. J. Ophthalmol. 66 (1982) 17–25, https://doi.org/10.1136/BJO.66.1.17.
[153] L. Bacakova, E. Filova, M. Parizek, T. Ruml, V. Svorcik, Modulation of cell adhesion, proliferation and differentiation on materials designed for body implants, Biotechnol. Adv. 29 (2011) 739–767, https://doi.org/10.1016/J.BIOTECHADV.2011.06.004.
[154] W. Song, J.F. Mano, Interactions between cells or proteins and surfaces exhibiting extreme wettabilities, Soft Matter 9 (2013) 2985–2999, https://doi.org/10.1039/C3SM27739A.
[155] C.F. Guimarães, L. Gasperini, A.P. Marques, R.L. Reis, The stiffness of living tissues and its implications for tissue engineering, Nat. Rev. Mater. 5 (2020) 351–370, https://doi.org/10.1038/s41578-019-0169-1.
[156] D.J. Moore, G.M. Clover, The effect of age on the macromolecular permeability of human bruch's membrane, Invest. Ophthalmol. Vis. Sci. 42 (2001) 2970–2975.
[157] C.J. Lee, J.A. Vroom, H.A. Fishman, S.F. Bent, Determination of human lens capsule permeability and its feasibility as a replacement for Bruch's membrane, Biomaterials 27 (2006) 1670–1678, https://doi.org/10.1016/J.BIOMATERIALS.2005.09.008.
[158] D.R. Lucas, M. Attfiled, J.B. Davey, Retinal dystrophy in the rat, J. Pathol. Bacteriol. 70 (1955) 469–474, https://doi.org/10.1002/path.1700700225.
[159] P.M. D'cruz, D. Yasumura, J. Weir, M.T. Matthes, H. Abderrahim, M.M. Lavail, et al., Mutation of the receptor tyrosine kinase gene Mertk in the retinal dystrophic RCS rat, Hum. Mol. Genet. 9 (2000) 645–651, https://doi.org/10.1093/hmg/9.4.645.
[160] M. Kondo, T. Sakai, K. Komeima, Y. Kurimoto, S. Ueno, Y. Nishizawa, et al., Generation of a transgenic rabbit model of retinal degeneration, Invest. Ophthalmol. Vis. Sci. 50 (2009) 1371–1377, https://doi.org/10.1167/iovs.08-2863.
[161] B.W. Jones, M. Kondo, H. Terasaki, C. Brock Watt, K. Rapp, J. Anderson, et al., Retinal remodeling in the Tg P347L rabbit, a large-eye model of retinal degeneration, J. Comp. Neurol. 519 (2011) 2713–2733, https://doi.org/10.1002/cne.22703.
[162] R. Obata, Y. Yanagi, Y. Tamaki, K. Hozumi, M. Mutoh, Y. Tanaka, Retinal degeneration is delayed by tissue factor pathway inhibitor-2 in RCS rats and a sodium-iodate-induced model in rabbits, Eye 19 (2005) 464–468, https://doi.org/10.1038/sj.eye.6701531.
[163] S.M. Ahn, J. Ahn, S. Cha, C. Yun, T.K. Park, Y.S. Goo, et al., Development of a post-vitrectomy injection of N-methyl-N-nitrosourea as a localized retinal degeneration rabbit model, Exp Neurobiol 28 (2019) 62–73, https://doi.org/10.5607/en.2019.28.1.62.
[164] H. Reisenhofer M, M. Balmer J, V. Enzmann, What can pharmacological models of retinal degeneration tell us? Curr. Mol. Med. 17 (2017) 100–107, https://doi.org/10.2174/1566524017666170331162048.
[165] J. Penn, D.M. Mihai, I. Washington, Morphological and physiological retinal degeneration induced by intravenous delivery of vitamin a dimers in rabbits, DMM Disease Models and Mechanisms 8 (2015) 131–138, https://doi.org/10.1242/dmm.017194.
[166] M.E. Pennesi, M. Neuringer, R.J. Courtney, Animal models of age related macular degeneration, Mol. Aspect. Med. 33 (2012) 487–509, https://doi.org/10.1016/j.mam.2012.06.003.
[167] B.V. Stanzel, Z. Liu, R. Brinken, N. Braun, F.G. Holz, N. Eter, Subretinal delivery of ultrathin rigid-elastic cell carriers using a metallic shooter instrument and biodegradable hydrogel encapsulation, Invest. Ophthalmol. Vis. Sci. 53 (2012) 490–500, https://doi.org/10.1167/iovs.11-8260.
[168] R.A. Brant Fernandes, F.R. Stefanini, P. Falabella, M.J. Koss, T. Wells, B. Diniz, et al., Development of a new tissue injector for subretinal transplantation of human embryonic stem cell derived retinal pigmented epithelium, Int J Retina Vitreous 3 (2017) 1–9, https://doi.org/10.1186/s40942-017-0095-6.
[170] R.C. Thomson, G.G. Giordano, J.H. Collier, S.L. Ishaug, A.G. Mikos, D. Lahiri-Munir, et al., Manufacture and characterization of poly(α-hydroxy ester) thin films as temporary substrates for retinal pigment epithelium cells, Biomaterials 17 (1996) 321–327, https://doi.org/10.1016/0142-9612(96)85570-0.